

AD-A043 061

STANFORD UNIV CALIF INST FOR PLASMA RESEARCH  
GEOMAGNETIC ACTIVITY: DEPENDENCE ON SOLAR WIND PARAMETERS.(U)  
MAY 77 L SVALGAARD

F/G 8/14

N00014-76-C-0207

UNCLASSIFIED

SU-IPR-699

NL

| OF |  
ADA043061



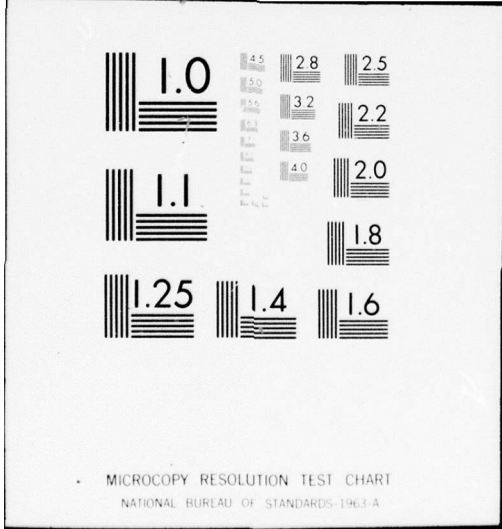
END

DATE

FILMED

9-77

DDC



ADA043061

①  
B.S.

# GEOMAGNETIC ACTIVITY: DEPENDENCE ON SOLAR WIND PARAMETERS

by  
**Leif Svalgaard**

Office of Naval Research  
Contract N00014-76-C-0207

National Aeronautics and Space Administration  
Grant NGR 05-020-559

National Science Foundation  
Grant ATM74-19007  
Grant DES75-15664

and  
The Max C. Fleischmann Foundation

DDC  
RECEIVED  
AUG 19 1977  
C

**SUIPR Report No. 699**

**MAY 1977**

Reproduction in whole or in part is permitted for  
any purpose of the United States Government.

DISTRIBUTION STATEMENT A  
Approved for public release  
Distribution Unlimited

AU NO. \_\_\_\_\_  
DDC FILE COPY



**INSTITUTE FOR PLASMA RESEARCH  
STANFORD UNIVERSITY, STANFORD, CALIFORNIA**

UNCLASSIFIED

SECURITY CLASSIFICATION OF THIS PAGE (When Data Entered)

REPORT DOCUMENTATION PAGE		READ INSTRUCTIONS BEFORE COMPLETING FORM
1. REPORT NUMBER SUIPR REPORT NO. 699	2. GOVT ACCESSION NO.	3. RECIPIENT'S CATALOG NUMBER
4. TITLE (and Subtitle) GEOMAGNETIC ACTIVITY: DEPENDENCE ON SOLAR WIND PARAMETERS.		5. TYPE OF REPORT & PERIOD COVERED Scientific, Technical
7. AUTHOR(S) Leif Svalgaard		6. PERFORMING ORG. REPORT NUMBER
9. PERFORMING ORGANIZATION NAME AND ADDRESS Institute for Plasma Research Stanford University Stanford, California 94305		8. CONTRACT OR GRANT NUMBER(S) N00014-76-C-0207
11. CONTROLLING OFFICE NAME AND ADDRESS Office of Naval Research Electronics Program Office Arlington, Virginia 22217		10. PROGRAM ELEMENT, PROJECT, TASK AREA & WORK UNIT NUMBERS
14. MONITORING AGENCY NAME & ADDRESS (if diff. from Controlling Office)		12. REPORT DATE May 1977
16. DISTRIBUTION STATEMENT (of this report) This document has been approved for public release and sale; its distribution is unlimited.		13. NO. OF PAGES 65
17. DISTRIBUTION STATEMENT (of the abstract entered in Block 20, if different from report)		15. SECURITY CLASS. (of this report) Unclassified
18. SUPPLEMENTARY NOTES TECH; OTHER		15a. DECLASSIFICATION/DOWNGRADING SCHEDULE
19. KEY WORDS (Continue on reverse side if necessary and identify by block number) Geomagnetic activity. Solar Wind. Magnetosphere. Semiannual variation. M-regions.		
20. ABSTRACT (Continue on reverse side if necessary and identify by block number) Current ideas about the interaction between the solar wind and the earth's magnetosphere are reviewed. The solar wind dynamic pressure as well as the influx of interplanetary magnetic field lines are both important for the generation of geomagnetic activity. The influence of the geometry of the situation as well as the variability of the interplanetary magnetic field are both found to be important factors. Semi-annual and Universal Time variations are discussed as well as the 22-year cycle in geomagnetic activity. All three are found to be explainable by the varying geometry of the interaction. Long-term changes in geomagnetic activity are reviewed.		

DDC  
 AUG 19 1977  
 REGISTERED  
 C

DD FORM 1473  
 1 JAN 73

EDITION OF 1 NOV 65 IS OBSOLETE

SECURITY CLASSIFICATION OF THIS PAGE (When Data Entered)

UNCLASSIFIED

332 630

GEOMAGNETIC ACTIVITY:  
DEPENDENCE ON SOLAR WIND PARAMETERS

By  
Leif Svalgaard

Office of Naval Research  
Contract N00014-76-C-0207

National Aeronautics and Space Administration  
Grant NGR 05-020-559

National Science Foundation  
Grant ATM74-19007  
Grant DES75-15664

and

The Max C. Fleischmann Foundation

SUIPR Report No. 699

May 1977

Institute for Plasma Research  
Stanford University  
Stanford, California

NTS	Work Sheet	<input checked="" type="checkbox"/>
DDO	8.11 Group	<input type="checkbox"/>
UNANNOUNCED		<input type="checkbox"/>
JUSTIFICATION		<input type="checkbox"/>
BY	DISTRIBUTION/AVAILABILITY GROUP	
Per.		

Chapter IX: Skylab Workshop Monograph on  
"Coronal Holes" (NASA)

GEOMAGNETIC ACTIVITY:  
DEPENDENCE ON SOLAR WIND PARAMETERS

by Leif Svalgaard

*Institute for Plasma Research  
Stanford University*

1. THE MAGNETOSPHERE

The magnetized collisionless solar wind plasma confines the magnetic field of the earth (and other solar system bodies) to a region around the planet called a magnetosphere. Alternatively we could say that the planetary magnetic field excludes the solar wind from the planetary environment. The confinement of the field or the exclusion of the solar wind plasma is not perfect, however. Due to particle gyration, the two plasma regimes overlap slightly thereby allowing significant mutual interaction. In spite of extensive efforts there is still no satisfactory physical theory of the interaction between the solar wind and the magnetosphere. In the broadest terms it seems that the magnetosphere may be described as a resistive - and therefore dissipative - element in an electrical circuit drawing its power from the kinetic energy of the streaming solar wind plasma. The tendency of a

plasma to react in highly dissipative - very often explosive - ways to any changes in boundary conditions is well-known from laboratory experiments and is also amply manifested in the magnetosphere as it continuously readjusts itself to the everchanging solar wind.

In a sense the magnetosphere is a continuing plasma physics experiment. The plasma parameters as well as the basic geometry of the experiment vary on many different time scales. Monitoring of the experiment is provided by observations of geomagnetic and auroral activity, and recently also by measuring directly the relevant external plasma parameters. It has been established that geomagnetic activity indeed can be used as a measure of solar wind parameters, and we are now in the position of being able to "calibrate" the experiment. It has long been recognized that "certain restricted areas of the Sun's surface are responsible for terrestrial magnetic disturbances" (Bartels, 1932) which then "yield supplementary independent information about solar conditions".

Penetration of a streaming plasma into a region of strong magnetic field may be considered to take place in a way lying between the following two extremes: 1) The plasma is completely diamagnetic and excludes the field from its interior by flowing around the field region, or 2) The plasma remains non-diamagnetic as it encounters the magnetic field and crosses it by means of an electric polarization and corresponding  $E \times B$  drift. The first viewpoint has been rather successfully used to account for the basic existence as well as for the approximate size and shape

of the magnetosphere, but fails in providing a physical basis for geomagnetic activity and disturbances. The second extreme seems to account for the behavior of laboratory plasma streams (e.g., Baker and Hammel, 1965) and may be applicable to the magnetosphere as well (Eastman *et al.*, 1976).

Consider a plasma stream moving into a strong uniform magnetic field normal to the plasma velocity vector. A schematic cross-section is shown in Figure 1. The effect of the Lorentz  $\vec{V} \times \vec{B}$  force is canceled by the action of an electric field  $\vec{E} = -\vec{V} \times \vec{B}$  that, if it is not already present, will be produced by a slight charge separation in the plasma caused by the Lorentz force deflecting ions and electrons in opposite directions. Now the plasma can move across the magnetic field due to the well-known  $\vec{E} \times \vec{B}$  drift. Electrostatic repulsion will tend to spread the polarization charge layers laterally along the magnetic field lines. If the field lines pass through a good conductor as shown in Figure 1, the polarization charge can be neutralized and the plasma stream will consequently be stopped or retarded. The depolarizing current along the field lines can thus serve to transfer momentum from the plasma stream to the conductor.

Figure 2 shows this model applied to the magnetosphere. As the solar wind plasma streams over the polar regions the dawn side of the magnetosphere becomes positively charged and the dusk side becomes negatively charged by the  $\vec{V} \times \vec{B}$  force. Depolarizing currents along high-latitude magnetic field lines close through the polar ionosphere hence imparting some of the solar wind momentum to the ionospheric

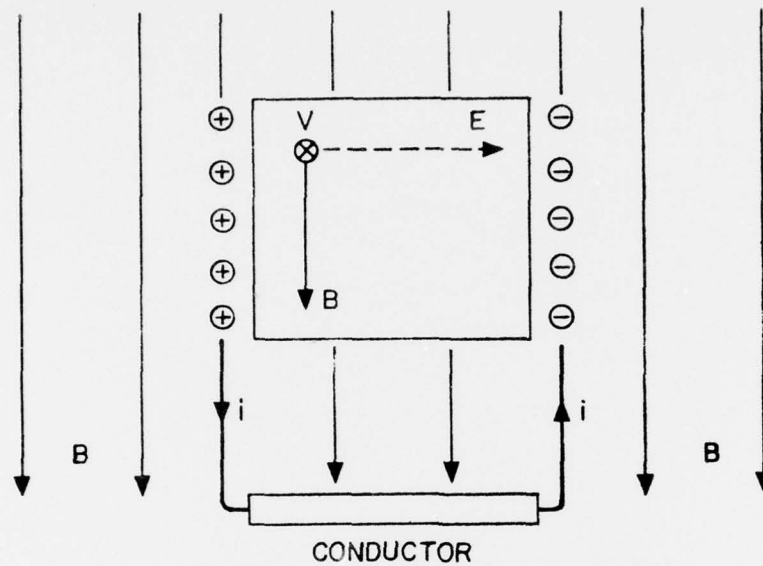


Figure 1. Schematic of a plasma stream moving into a transverse magnetic field  $B$ . The polarization electric field  $E = -\vec{V} \times \vec{B}$  follows from a charge separation in the plasma. The charge layers can spread along magnetic field lines (the current  $i$ ) and may be neutralized if a good conductor connects the two spreading charge layers.

and magnetospheric plasma and producing a magnetospheric boundary layer of retarded solar wind plasma. The geomagnetic field lines through the boundary layer become stretched downstream forming the magnetotail. Thus, the magnetosphere acts like a magnetohydrodynamic generator, converting kinetic energy of

moving plasma into electrical energy which then ultimately is dissipated within the magnetosphere or in the boundary layer. When the northern and southern parts of the boundary layer meet downstream of the earth, plasma regions with oppositely directed magnetic field lines are brought together and may reconnect explosively. The resulting "magnetospheric fireball" (Frank *et al.*, 1976) is a source of energetic particles which, if precipitated into the earth's atmosphere, produce the often spectacular auroral displays associated with geomagnetic disturbances.

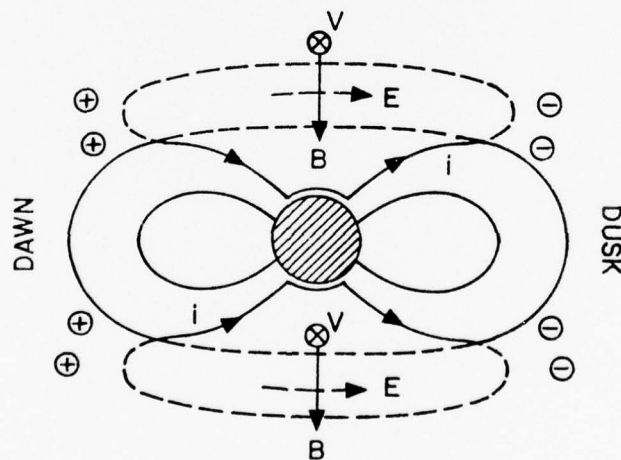


Figure 2. The model shown in Figure 1 as applied to the magnetosphere. Depolarizing currents along high-latitude magnetic field lines close through the polar ionosphere.

In this view of the solar wind - magnetosphere interaction, geomagnetic activity is considered to be the magnetic effects of currents around and above the earth (which may in turn induce currents inside the earth). These currents are partly associated with the depolarization of the magnetospheric boundary layer but to an even greater and more important extent they are induced by rapidly changing magnetic field configurations (*e.g.* in magnetospheric fireball events) as the stressed magnetosphere gives way and relaxes to a lower energy state. As the basic interaction is transfer of momentum from the solar wind to the magnetospheric and ionospheric plasma, we would quite generally expect that geomagnetic activity should increase with increasing momentum flux of the solar wind impinging on the earth's magnetic field. Any further solar wind parameters that could enhance the coupling to the magnetosphere might similarly be responsible for additional enhancement of geomagnetic activity.

## 2. RELEVANT PARAMETERS OF THE SOLAR WIND - MAGNETOSPHERE INTERACTION

The initial entry of solar wind onto geomagnetic field lines seems to depend on the direction of the interplanetary magnetic field (Cole, 1974; Bahnsen and Hansen, 1976). In fact, the boundary layer is observed to be much thicker at times when the interplanetary magnetic field has a large southward component (Sckopke *et al.*, 1976). Over regions of the magnetopause where the magnetic fields outside and

inside the boundary are parallel, plasma flow is permitted across the boundary entailing an electric field tangential to the magnetopause. A plasma particle that has an initial guiding center velocity, carrying it across a boundary between magnetic fields of different direction, will continue its motion when the two fields have a parallel component but will be reflected back when the magnetic fields on either side of the boundary have an anti-parallel component. In loose terms we may say that the solar wind plasma can penetrate deeper into the geomagnetic field at places where the field direction is the same as the direction of the interplanetary magnetic field embedded in the solar wind because it takes longer for the plasma to realize that something is wrong. For anti-parallel fields, initial drifts towards the boundary actually result in a removal of plasma from the opposing magnetic field lines. As pointed out by Cole (1974) this will tend to cause vacuum connection or merging of geomagnetic and interplanetary magnetic field lines. Vacuum connection is not associated with electric fields or particle energization. Turning a toy magnet in the earth's magnetic field causes a continuing change of the topology of the field around the toy magnet without electrical effects. Solar wind plasma can now enter the magnetosphere along the newly connected field lines as they are convected downstream and thus increase the thickness and extent of the boundary layer. There is experimental evidence that both the cross-field diffusion and the magnetic merging discussed above are operating simultaneously (Reiff *et al.*, 1977). In addition to the thickening

of the boundary layer, magnetic flux is also being transferred from the dayside magnetosphere to the tail region by the merging process. This in turn leads to increased frequency and intensity of re-connective events within the downstream magnetosphere resulting in enhanced geomagnetic activity.

The number of interplanetary magnetic field lines that are brought up to the magnetosphere per unit time and unit area depends on the product of the magnetic flux density  $B$  and the solar wind speed  $V$ . A geometrical factor depending on the angle between the interplanetary magnetic field and the geomagnetic field determines how much of the flux can merge. This factor is largest when the two fields are antiparallel at the front of the magnetopause and decreases to zero for exactly parallel fields. Observations (Fairfield, 1967) show that the interplanetary magnetic field is "draped" around the nose of the magnetosphere as shown in Figure 3. The draping does not change the latitude angle of the field significantly. The result is then that the magnetic field just outside the magnetopause is tangential to the magnetosphere surface - directed from dawn to dusk in case of an ideal "away" polarity interplanetary magnetic field and from dusk to dawn in case of toward polarity. In addition the field may make a non-zero latitude angle with the ecliptic. We note that for negative latitude angles (southward fields) conditions are favorable for merging at the nose of the magnetosphere and also favorable for cross-field diffusion into the magnetosphere over the polar regions.

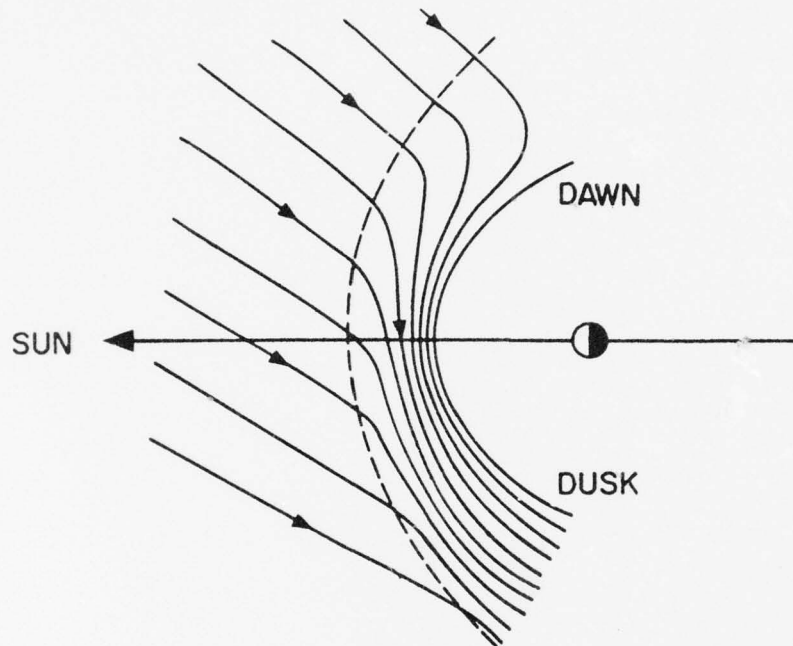


Figure 3. Equatorial plane view of the observed draping of the interplanetary magnetic field around the nose of the magnetosphere. The situation is shown here for "away" polarity. the main effect is that the interplanetary magnetic field at the dayside magnetosphere is largely parallel to the magnetopause.

The geomagnetic dipole is roughly perpendicular to the solar wind velocity vector (implied in Figure 2). Qualitatively, it seems reasonable that the exclusion of solar wind plasma from the terrestrial environment depends in some way on the angle  $\psi$  between the solar wind flow direction and the dipole axis because the magnetic field seen by the solar wind is weakest

when  $\psi = 90^\circ$ . The angle  $\psi$  varies both seasonally ( $90^\circ \pm 23^\circ.5$ ) and diurnally ( $\pm 11^\circ.5$ ) due to the  $23^\circ.5$  angle between the earth's equator and the ecliptic and because the dipole axis is inclined  $11^\circ.5$  to the rotation axis. It is thus likely that such variations of the geometry of the magnetospheric "plasma physics experiment" could influence the coupling efficiency. There are, in fact, observed variations in the amount of geomagnetic activity that closely follow variations of the dipole inclination  $\psi$ . These are first of all the classical semi-annual variation of the activity, first recognized by Sabine (1856), and secondly the Universal Time variation found by McIntosh (1959). Geomagnetic activity seems to be largest when the dipole axis is perpendicular to the solar wind flow direction.

We have identified several solar wind - magnetosphere parameters that are important for the generation of and possibly modulation of geomagnetic activity. In the following summary we discuss how fundamental properties of the solar wind enter into the geomagnetically active parameters.

- 1) The density of the solar wind momentum flux (the dynamic pressure) is given by  $\rho V^2$  where  $\rho$  is the mass density and  $V$  is the solar wind speed. Often the proton number density,  $n$ , is used as a parameter largely proportional to  $\rho$ . The Helium content of the solar wind varies and can at times be quite high and contribute significantly to  $\rho$ .
- 2) The influx of merging interplanetary magnetic field lines is  $BV$  per unit length across the nose of the magnetosphere times a geometrical factor

$q(\alpha)$  where  $\alpha$  is the angle between the directions of the draped interplanetary field and of the geomagnetic field at the dayside magnetopause (see also Figure 18). The quantity  $B$  is the magnitude of the interplanetary magnetic field. The geometrical factor also includes the variation of the efficiency of cross-field diffusion of solar wind plasma with the angle  $\alpha$ . It is worth pointing out that merging and cross-field diffusion takes place in different regions on the dayside magnetopause but that they both depend in approximately the same way on  $\alpha$ .

3) As geomagnetic activity and solar wind parameters often are expressed as time averages over some interval, e.g. one hour or three hours, and since the relations between them are non-linear in many cases, the variability of the solar wind must be taken into account. This is particularly important for the direction of the interplanetary magnetic field. It has been suggested that the variability itself may contribute to geomagnetic activity (Holzer and Reid, 1975). Because the time fluctuations are most pronounced for the *direction* of the interplanetary magnetic field, the following ratio will be taken as a measure of solar wind variability on the time scale involved (a few hours):  $f = \sigma_F/B$ , where

$$\sigma_F^2 = \sigma_X^2 + \sigma_Y^2 + \sigma_Z^2 \quad (1)$$

is the total variance computed as the sum of the variances for each component of the interplanetary magnetic field.

4) Finally we remark that the geometry of a dipolar magnetic field involves the "colatitude"  $\psi$  in the form  $(1 + 3 \cos^2 \psi)$  which enters into the semi-empirical description of the variation of activity with the dipole inclination  $\psi$ .

The ideal way of studying a phenomenon that depends on several parameters would be to let only one parameter vary at a time. This ideal can often be simulated if enough observational data is available by grouping the data into several classes in such a way that within each class there is only a slight variation of all the parameters. The number of classes may be decreased if some of the parameters are uncorrelated (or only weakly correlated) in which case average values of these parameters can be used. We shall employ the grouping technique extensively in the present study.

### 3. GEOMAGNETIC ACTIVITY

About one sunspot cycle worth of interplanetary solar wind data is available through the National Space Science Data Center (e.g., King, 1976). This includes both magnetic field data and plasma data. To characterize geomagnetic activity, an index measuring the degree of disturbance is commonly used. A great variety of geomagnetic indices have been proposed and employed over the years; some of them are specialized indices designed to characterize specific aspects of the total disturbance field while others are meant to be global or 'planetary' indices giving a measure of

the worldwide level of magnetic disturbances (Siebert, 1971; Mayaud, 1967, 1968, 1972; Svalgaard, 1976). In the following section we discuss the meaning of the geomagnetic index  $am$  that will be used in the present investigation. Although the actual derivation of such indices is a highly specialized subject, it is my experience that enough misconception and confusion exist about what geomagnetic activity is and how it is measured to warrant a somewhat tutorial approach (for complete details see Mayaud, 1967).

Figure 4 shows a reproduction of a magnetogram of the variation of the horizontal component of the geomagnetic field at a mid-latitude station. The record extends over twelve three-hour Universal Time intervals. A geomagnetic storm begins about 9<sup>h</sup> on the first day and the field level the following night is strongly depressed relative to the level on the previous night. A regular daily variation is indicated by a dashed line as far as it can be determined from the undisturbed portion of the record and from the observer's knowledge of what the typical daily variation generally looks like for the station during the season (and lunar phase) in question. Winds and tides in the ionosphere are responsible for producing these rather regular - but nevertheless varying from day to day - excursions of the geomagnetic field. During each three-hour interval some irregular field variations appear in the record. They have an absolute maximum and an absolute minimum within the interval; part of this variation is due, however, to the regular daily variation and must be eliminated. Graphically, this corresponds to the measurement of the vertical dis-

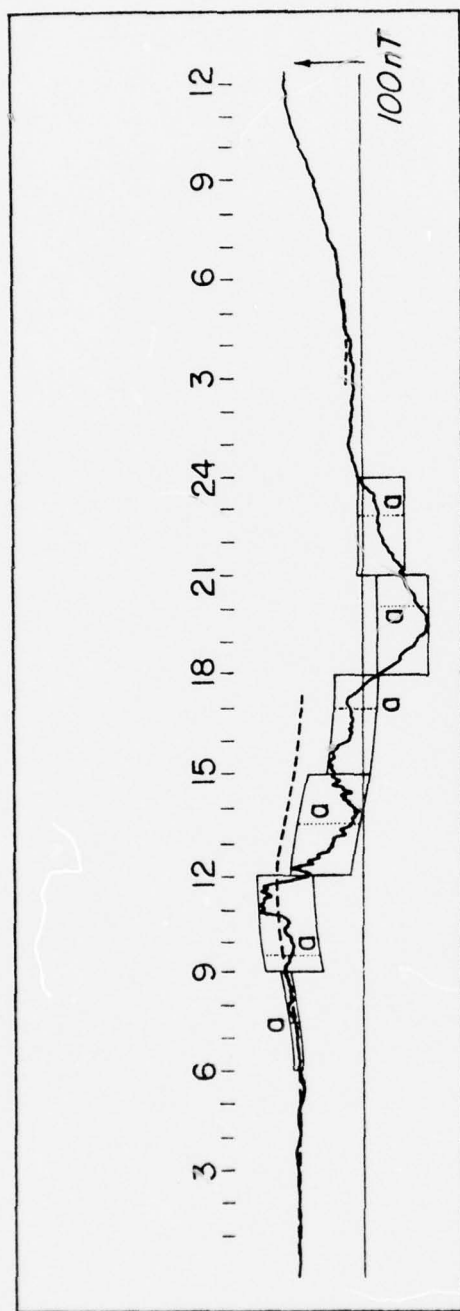


Figure 4. Magnetogram of the horizontal component of the geomagnetic field at a mid-latitude station. The record extends over twelve three-hour intervals. A magnetic storm begins around 9<sup>h</sup> universal time. Dashed lines show the estimated daily variation. For several three-hour intervals the amplitude,  $\alpha$ , of the activity is illustrated (after Mayaud, 1967).

tance between two curves parallel to the daily variation and enclosing the irregular variations. Several such amplitudes have been marked on Figure 4. It is important to emphasize that what is measured is *not* the deviation from some "quiet" reference level but an *amplitude* of fluctuations believed to be caused by the solar wind interacting with the magnetosphere during that three-hour interval. Finally, to construct a global or planetary index, amplitudes are averaged over selected observatories with as far as possible a uniform distribution in longitude in both the northern and the southern hemisphere. The details of the final computation (Siebert, 1971; Mayaud, 1968) need not concern us here; we only note that several indices exist because of differences in stations used and in time periods covered. Since 1959 the station distribution has been uniform enough to allow computation of a very close approximation to a truly global index: the am-index (Mayaud, 1968). the 'm' in am stands for *mondial*, the French word for worldwide. An earlier index, the well-known ap-index, (p = planetary) extends back to 1932 but is based on an inferior station distribution. Using two antipodal observatories it has been possible to construct a homogeneous series of activity amplitudes going back to 1868: the aa-index (Mayaud, 1972).

From the three-hour indices, daily indices can be computed. E.g., the Ap-index is the average ap-index over the UT-day. Expressing the Ap-index on a quasi-logarithmic scale from 0 to 9 gives a very compact representation of geomagnetic activity on a daily basis: the C9-index. The choice of a three-hour index as the basic activity measure is mainly dictated by the fre-

quency-spectrum of the irregular variations and may be justified on physical grounds because three hours is the time it takes the solar wind to pass the magnetotail. The magnetosphere usually reacts to a change in boundary conditions in a time considerably smaller than three hours so that no time delay is necessary when comparing interplanetary data with the am- or ap - indices.

#### 4. INFLUENCE OF BULK PROPERTIES OF THE SOLAR WIND

That geomagnetic activity indeed does depend on solar wind parameters, especially solar wind speed, was noted in the very earliest studies of the influence of the solar wind (Snyder *et al.*, 1963), and has been extensively confirmed since. Figure 5 shows that on the average, the am-index is approximately proportional to the square of the solar wind speed  $V$ . It is somewhat remarkable that an index that was conceived almost forty years ago (Bartels, 1938) responds so clearly to an extra-terrestrial quantity. A vivid illustration of this relationship on a day-by-day basis is given by Sheeley *et al.* (1977). As we shall show, the relationship is really a complex one; several physical causes cooperate to give the overall effect. As the first step towards this goal we consider separately the possible influences of the influx of interplanetary magnetic field lines,  $BV$ , and of the solar wind flux,  $nV^2$ . Averages of the am-index computed for rather narrow bins or intervals of both  $BV$  and  $nV^2$  are shown in Figure 6. We assume - and have actually veri-

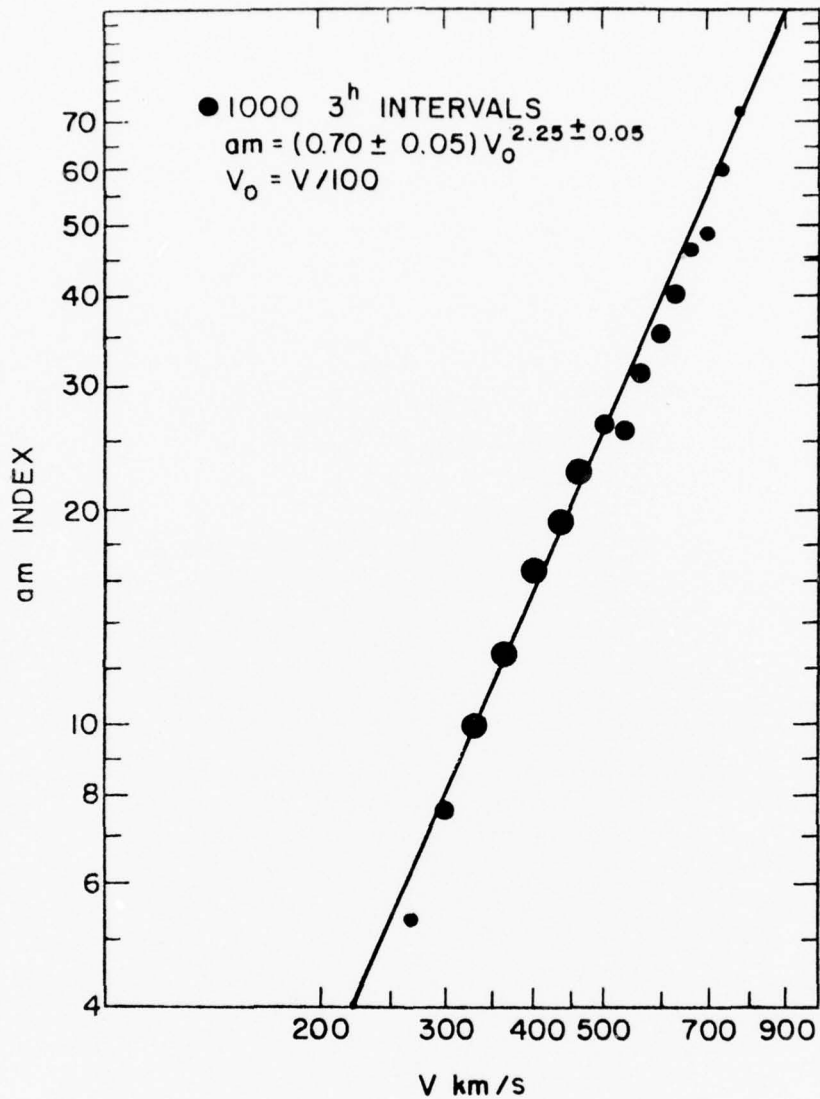


Figure 5. Average dependence of the am-index on the solar wind speed  $V$  using data from the interval 1965-1973. More than 9000 three-hour intervals of data are available. The area of the filled circles are proportional to the number of three-hour intervals used in the average. For the larger datapoints the statistical uncertainty of the average is less than the dia-

meter of the circles. For an average over 100 three-hour intervals the error is of the order of 10% of the average values. A power-law dependence is suggested by the data with an exponent near 2.25. Similar results have been reported by Murayama and Hakamada (1975) and by Crooker and Feynman (1977).

fied - that values of other solar wind parameters have approximately the same distribution in each bin. This is especially important in the case of the direction of interplanetary magnetic fields. Note that a doubling of BV also doubles the average am-index but that it is necessary to increase  $nV^2$  by a factor of 7 or 8 in order to obtain a doubling of am. The figure suggests the following approximate relationship

$$am \sim BV \cdot (nV^2)^{1/3} \quad (2)$$

implying that both the magnetic flux and the momentum flux are important at the same time for the generation of geomagnetic activity. To eliminate the possibility that mutual correlations between V, B and n cooperate to produce this apparent relationship, we now examine only data with almost constant values of all parameters except n and B.

In the first case we ask the question: If the number density, n, is the only parameter allowed to vary, does the am-index vary as the one-third power of n? As shown in Figure 7, that seems indeed to be the case within observational accuracy. A similar analysis

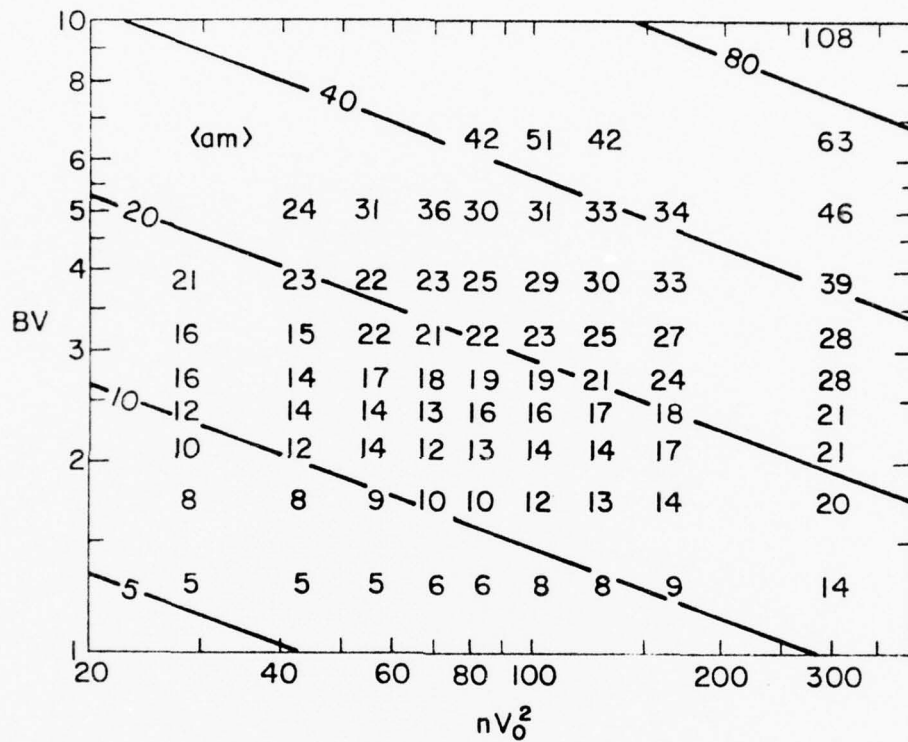


Figure 6. Average values of the am-index for different ranges of the flux of interplanetary magnetic field lines, BV, and of the solar wind momentum flux  $nV_0^2$ . The unit for BV in this figure is millivolt/meter. The number density  $n$  is given in protons/cm<sup>3</sup> and  $V_0$  denotes the solar wind speed divided by 100:  $V_0 = V/100$ , with  $V$  expressed in km/s. Each value on the plot represents an average of about 100 cases. Straight lines have been drawn corresponding to the relation given by eq.(2).

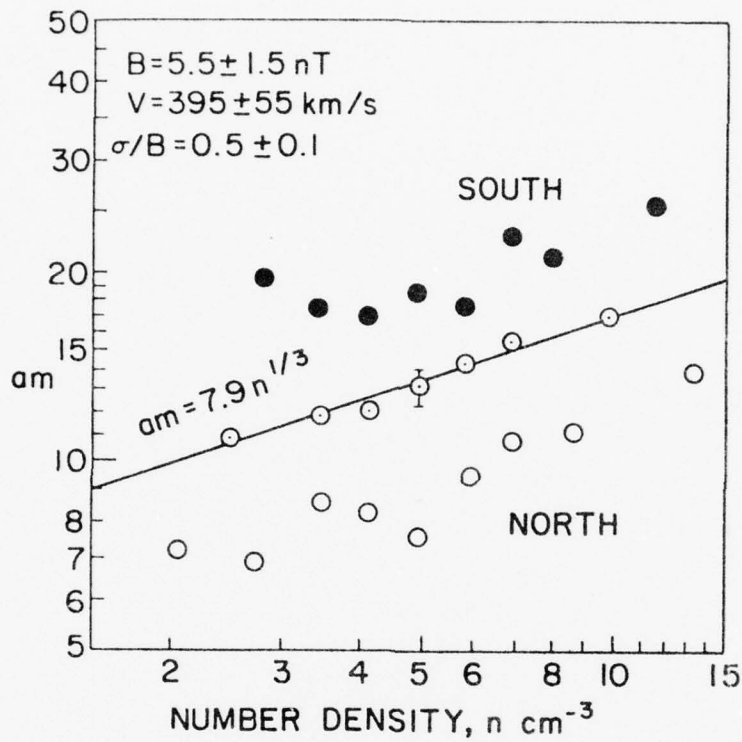


Figure 7. The dependence of  $am$  on the number density,  $n$ , for almost constant values of all the other solar wind parameters. Filled circles represent cases where the interplanetary magnetic field was largely southwards with respect to the geomagnetic field (*i.e.*  $\cos\alpha < -0.25$ ); open circles represent cases of predominantly northwards fields ( $\cos\alpha > +0.25$ ), while circles with a dot represent cases of interplanetary fields largely perpendicular to the geomagnetic dipole. A typical error bar is shown in the center of the figure.

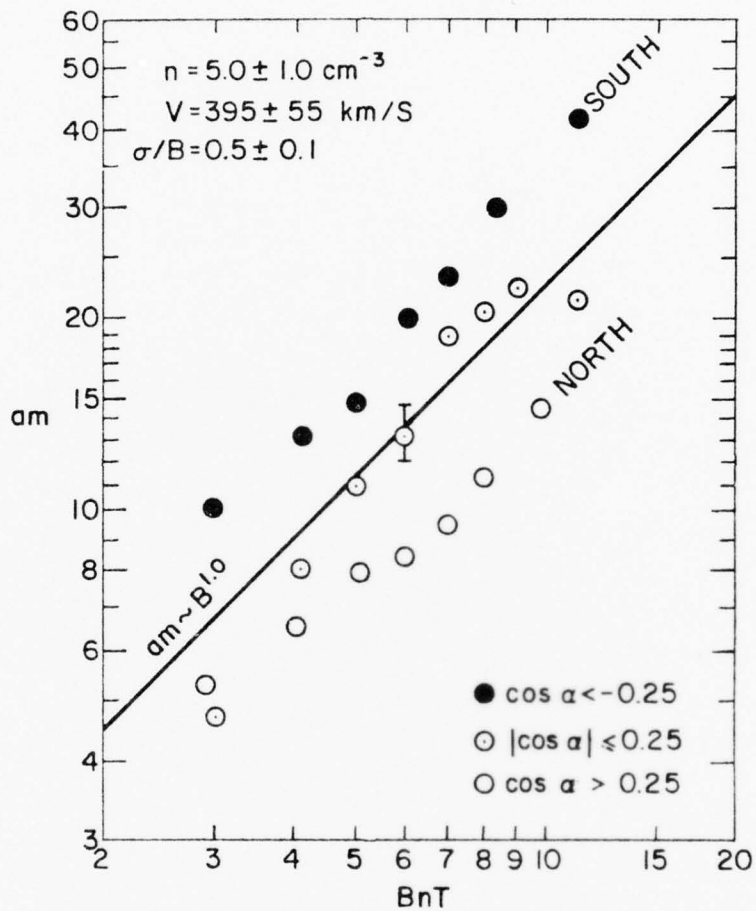


Figure 8. Similar to Figure 7 but in this case the field magnitude B is used as the independent variable. In both Figures 7 and 8 the selected ranges of solar wind parameters are shown in the upper left-hand corner.

for the magnetic field strength,  $B$ , is shown in Figure 8, confirming the first-power dependence. In both figures a further subdivision according to the angle,  $\alpha$ , between the direction of the geomagnetic field on the dayside magnetosphere and of the interplanetary magnetic field was performed. The data seems to be consistent with a first-power dependence on  $B$  and a one-third power dependence on the number density  $n$ . The relationship eq.(2) indicates that the influences of those two parameters are not independent -- in that case the effects would be additive rather than multiplicative. In addition it is apparent that the direction of the interplanetary magnetic field is of paramount importance and that its influence can be described as a modulating angle-dependent *factor* that should be incorporated into eq.(2) - because of the roughly parallel sequences of datapoints in both Figures 7 and 8.

That geomagnetic activity correlates very well with  $BV$  times a function  $q(\alpha)$  of the angle  $\alpha$  between the interplanetary and the geomagnetic field is well-known and generally accepted (e.g., Burton *et al.*, 1975; Crooker, 1975). In fact, one of the outstanding current problems in the study of the magnetosphere is to understand the physics of that correlation. By forming the ratio  $am/BV$ , we get a quantity that is reduced for the influence of  $BV$  and thus might show a clearer correlation with the momentum flux  $nV^2$ . The result is shown in Figure 9. A physical interpre-

tation of this relationship might be that the magnetosphere is powered by solar wind kinetic energy, but that the power input is strongly controlled by coupling via the interplanetary magnetic field.

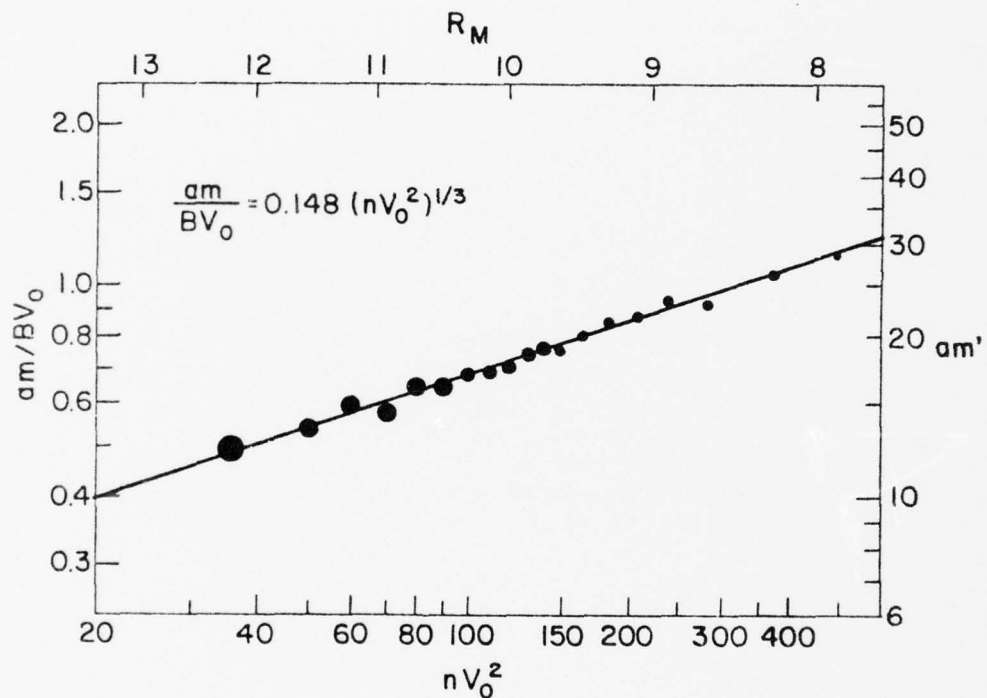


Figure 9. By dividing the am-index by BV we isolate the influence due to  $nV^2$ . In this figure,  $am/BV_0$  is plotted against  $nV_0^2$  (where  $V_0 = V/100$ ) confirming the one-third power dependence suggested in Figure 7. The areas of the filled circles are proportional to the number of data values in each average. A total of more than 9000 three-hour intervals were available for the analysis.

## 5. INFLUENCE OF GEOMETRICAL FACTORS

Further insight into the coupling problem can be gained by performing the same type of analysis as in Figure 9 for various subsets of the data characterized by different ranges of the relevant parameters such as the angle  $\alpha$  between the two fields, the relative variability  $f$  and the angle  $\psi$  between the solar wind flow and the earth's dipole axis. Figures 10, 11 and 12 display the results. The effect of varying the angle  $\alpha$  is by far the most important (Figure 10), although significant increase in activity is also associated with high variability of the interplanetary magnetic field (Figure 11). Finally there is a small but persistent tendency for activity to be higher when the geomagnetic dipole is perpendicular to the solar wind flow direction (Figure 12). The consistent trends in these Figures strongly suggests that we may largely remove the influence of  $BV$  and  $nV^2$  simply by computing a reduced am-index:

$$am' = am \left( \frac{\langle BV \rangle}{BV} \right) \left( \frac{\langle nV^2 \rangle}{nV^2} \right)^{1/3} \quad (3)$$

We have used  $\langle BV \rangle = 2100$  and  $\langle nV^2 \rangle = 1.05 \times 10^6$  (B in nT, V in km/s, and n in protons/cm<sup>3</sup>). To investigate the effect of  $\alpha$  and of the relative variability  $f$  in detail, the data is divided into groups according to the value of  $f$ . The group characterized by  $f = 0.5$  will consist of all data values for which  $f$  lies between 0.45 and 0.55, and so forth. Then for each group we make a further subdivision according to the value of  $\cos \alpha$ . There is enough data to allow a bin-

width of 0.1 in  $\cos \alpha$  without compromising the accuracy of the mean value of the am-index computed for every subdivision. Figures 13 and 14 show the result.

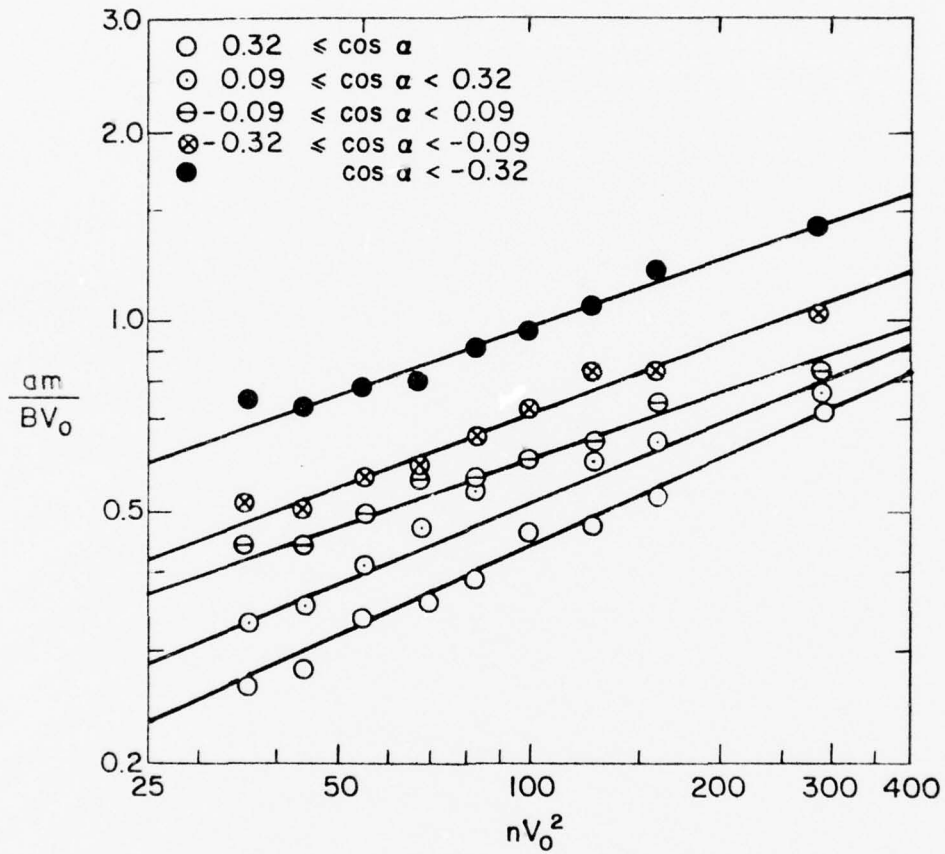


Figure 10. Similar in format to Figure 9, except with a further subdivision of the data into five classes of different orientation of the interplanetary magnetic field; from mostly southwards (filled circles) turning to mostly northwards (open circles). The class intervals selected for  $\cos \alpha$  are shown in the upper left corner.

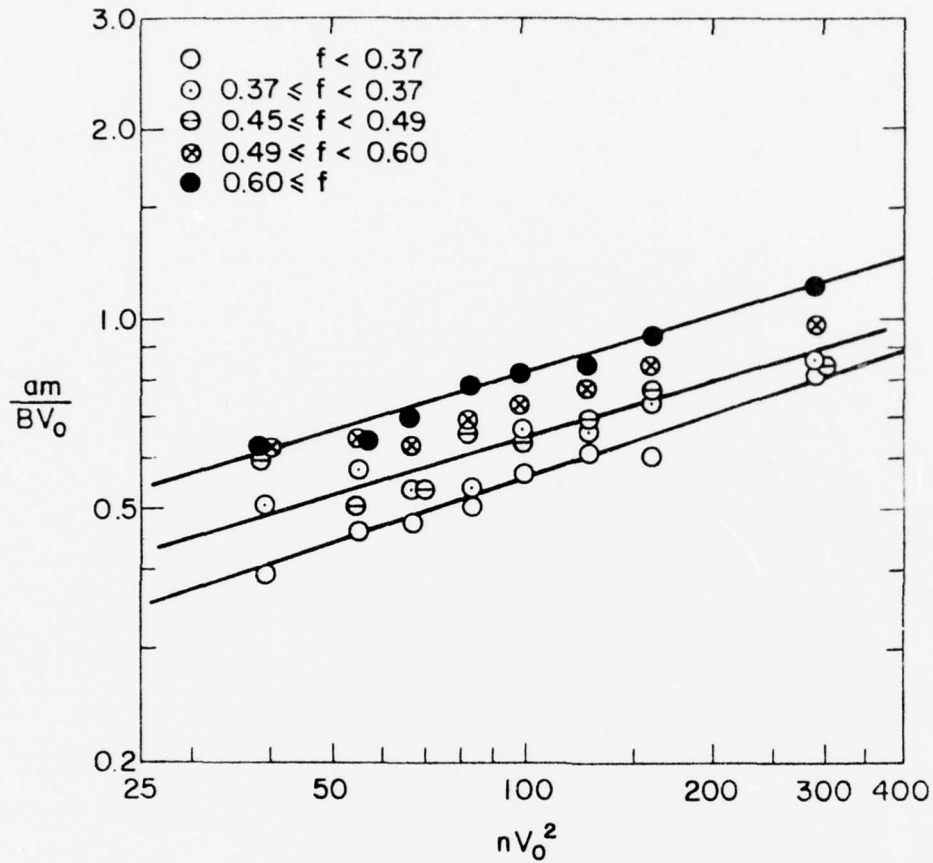


Figure 11. Similar to Figure 10, except that the data was divided according to the relative variability  $f = \sigma/B$  of the interplanetary magnetic field. The classes range from quiet ( $f < 0.37$ ; open circles) to disturbed ( $f \geq 0.60$ ; filled circles) conditions. Note that the time scale for determination of  $f$  is three hours. If the field magnitude was constant (very nearly true) within a three-hour interval the maximum value of  $f$  would be 1.

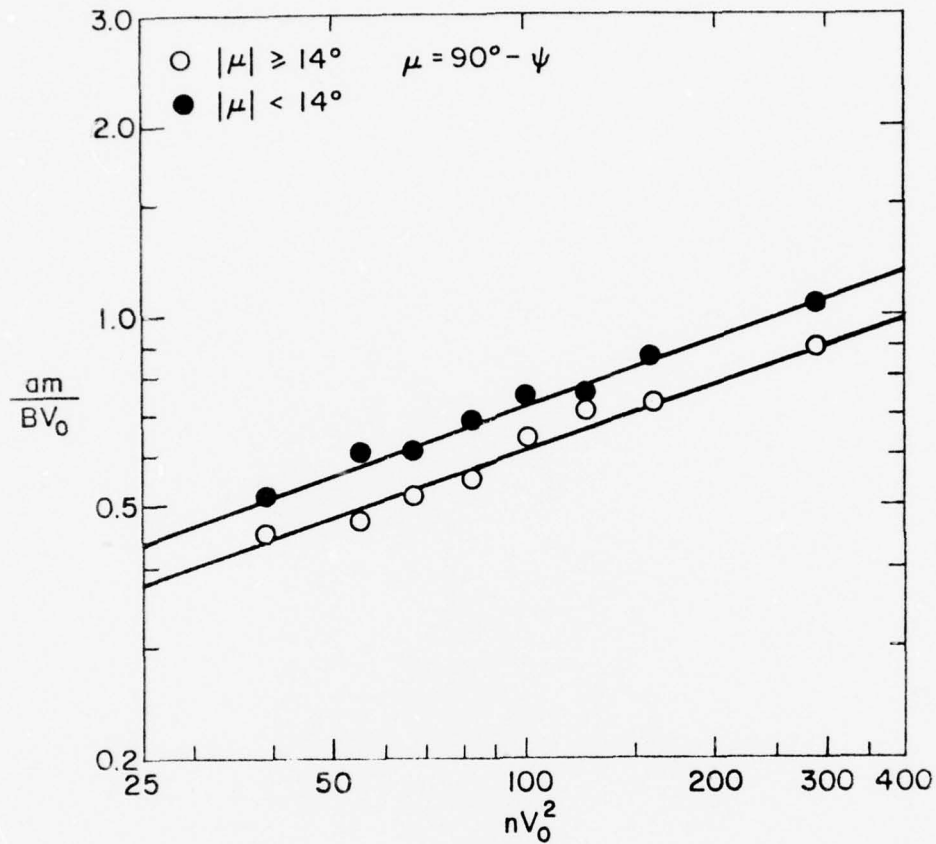


Figure 12. Similar to Figure 11, except that the data was divided in two classes according to whether the tilt angle ( $\mu=90^\circ-\psi$ ) of the geomagnetic dipole was numerically less than  $14^\circ$  (filled circles) or greater than  $14^\circ$  (open circles). There is clearly a persistent tendency for activity to be higher when  $\mu$  is small, *i.e.* when the dipole is nearly perpendicular to the solar wind flow direction.

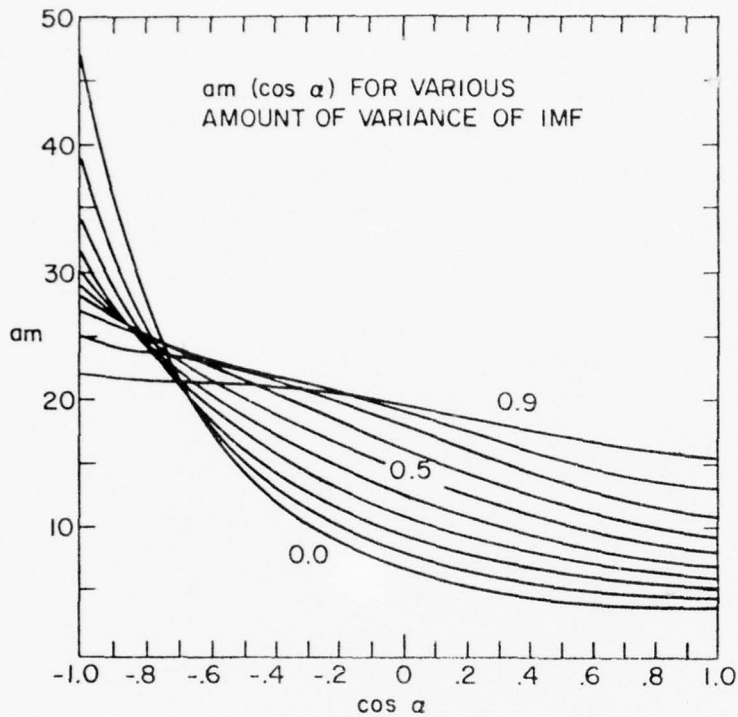


Figure 13. The dependence of geomagnetic activity ( $am$ -index reduced for  $BV$  and  $nV^2$  influence, see text) on  $\cos\alpha$ , where  $\alpha$  is the angle between the geomagnetic field lines at the nose of the magnetosphere and the average interplanetary magnetic field during the three-hour interval corresponding to  $am$ . Draping (Figure 3) of the interplanetary field is assumed and the reader is referred to Figure 18 for a precise definition of  $\alpha$ . Several curves are shown for various values of the relative variability  $f$ ; from  $f = 0.0$  to  $f = 0.9$  as labeled on the figure. Note the very flat curves for high variability and the steeply falling curves for low variability of the interplanetary field.

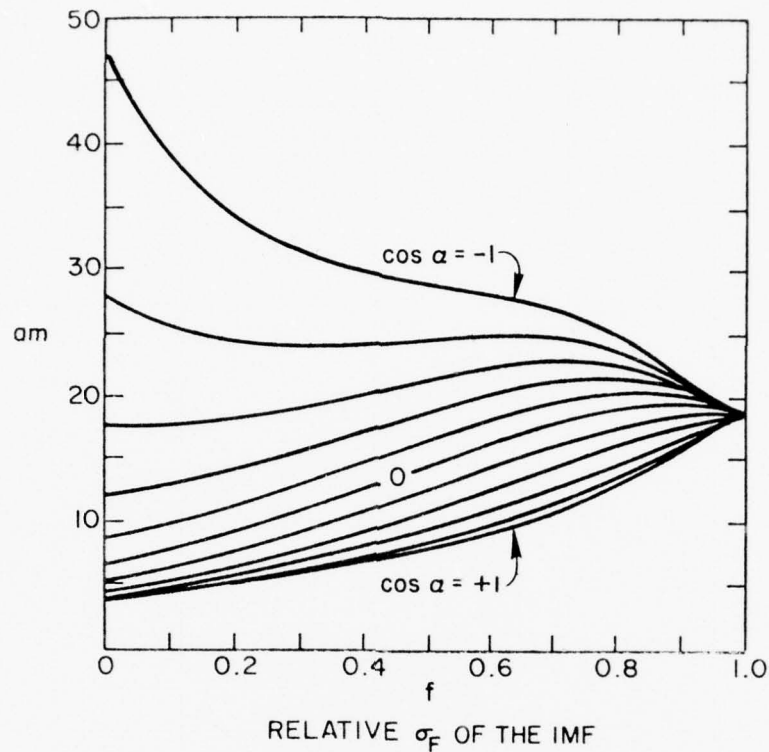


Figure 14. Dependence of reduced am-index on the relative variability  $f$  of the interplanetary magnetic field for several values of cosine of the angle  $\alpha$  between the interplanetary field and the geomagnetic field. Note that for most values of  $\alpha$  activity increases with increasing variability, but that for nearly southwards fields the inverse is the case. The curve labeled 0 is for  $\cos\alpha = 0$  which is the most probable value of  $\cos\alpha$  and is thus indicative of the typical situation. Figure 16 shows some of the individual data points used to construct the smooth curves in Figures 13 and 14.

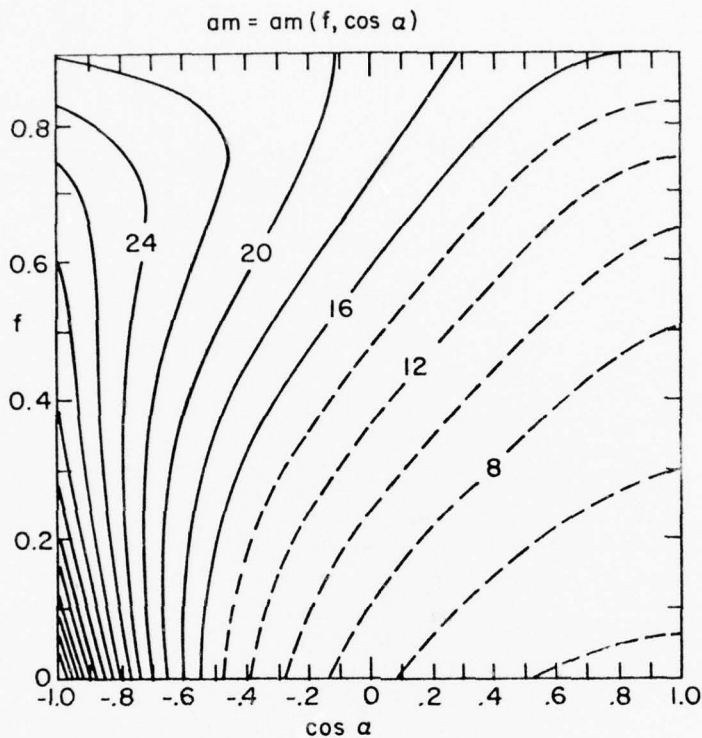


Figure 15. Actually Figures 13 and 14 are synthesized from this figure. Bins of  $\cos \alpha$ , (0.1 wide) and bins of  $f$  (0.1 wide) were formed and the average value of reduced  $am$  was computed for each bin. The figure shows a contourplot of the results. Contour levels less than average are shown as dashed lines. It is now a simple matter to construct the curves in Figures 13 and 14. The following fourth-order polynomial fit to the contours gives synthetic  $am$ -values that have a very high correlation (0.992) with the observed averages for each bin:

$$am = 6.6 \exp(-1.275 \cos \alpha + 1.815f + 0.565 \cos^2 \alpha + 2.041f \cos \alpha - 0.642f^2 - 0.001 \cos^3 \alpha - 1.877f \cos^2 \alpha - 2.715f^2 \cos \alpha + 0.636f^3 + 0.118 \cos^4 \alpha + 0.081f \cos^3 \alpha + 1.190f^2 \cos^2 \alpha + 1.935f^3 \cos \alpha - 0.754f^4)$$

The above formula expresses a purely formal relationship, of course.

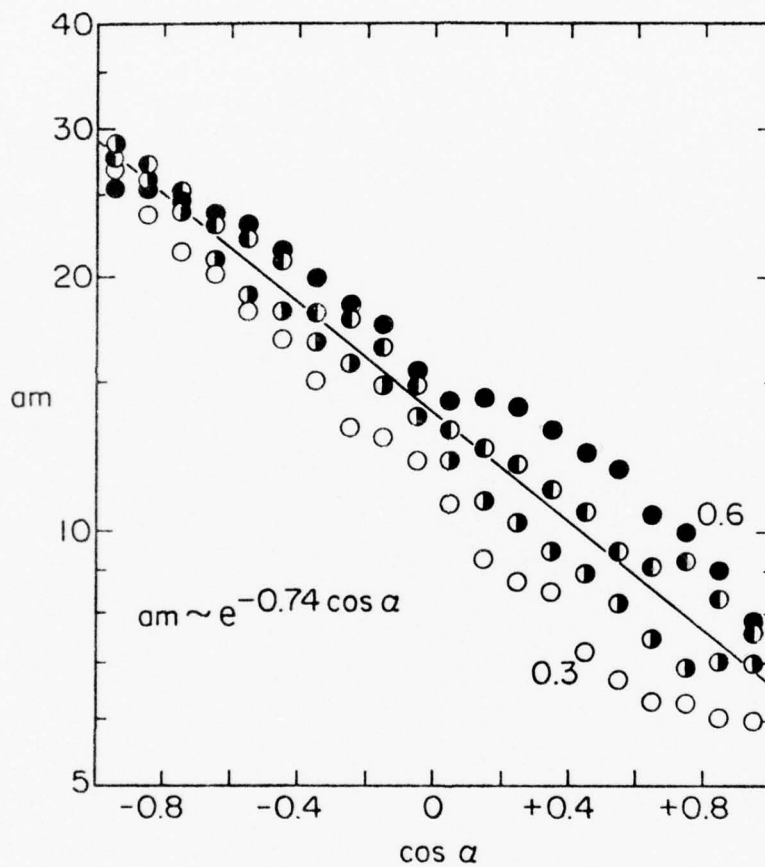


Figure 16. Reduced  $am$  as a function of  $\cos \alpha$  for  $f = 0.3$  (open circles),  $f = 0.4$  (circles open on the left),  $f = 0.5$  (circles filled on the left), and  $f = 0.6$  (filled circles). The scale for  $am$  is logarithmic. An expression of the form  $am = k \exp(-g \cos \alpha)$  fits the data.

Each curve in Figure 13 is drawn through the average points for each  $f$ -group and shows how the activity varies with  $\alpha$  for that particular variability of the interplanetary magnetic field. In Figure 14 we show how the activity varies with the variability  $f$  for different values of  $\cos\alpha$  ranging from  $-1$  to  $+1$ , *i.e.* from southwards to northwards.

We note first that when the variability is high (*e.g.*,  $f = 0.9$ ) geomagnetic activity is almost independent of  $\alpha$ . The reason is, of course, that the average direction of the interplanetary magnetic field during the three-hour interval in question is undefined or nearly so. With decreasing variance the importance of southwards fields ( $\cos\alpha < 0$ ) becomes more and more prominent. For  $f = 0$  the curve rises sharply as  $\cos\alpha$  approaches  $-1$ . In discussing the physics of this relation we should bear in mind that the interplanetary magnetic field at the magnetopause fluctuates more than the field in interplanetary space due to passage through the bow-shock of the magnetosphere. This suggests that the curve showing am-index dependence on  $\cos\alpha$  extrapolated to zero variability of the field at the magnetopause would rise even sharper than the curve labeled  $f=0$  in Figure 13. The implication seems to be that the coupling to the solar wind due to magnetic field connection is very weak unless the geometry is very favorable, *i.e.* the external field is almost anti-parallel to the dayside geomagnetic field. Due to ever-present fluctuations of the interplanetary magnetic field - considerably enhanced after passage through the bow-shock - favorable conditions for connection

occur often enough within a three-hour interval at so many places on the magnetopause as to give the impression that reconnection and hence geomagnetic activity occur for all orientations of the interplanetary magnetic field and varying in efficiency smoothly from a maximum for anti-parallel fields to a non-vanishing minimum for parallel fields.

A simple computer simulation can qualitatively reproduce the curves in Figures 13 and 14 starting with the  $f = 0$  curve and by just varying the three components of the interplanetary field such as to result in a certain average vector making the angle  $\alpha$  with the geomagnetic field. By adjusting the time scale of the computer generated variations, any relative variability  $f = \sigma/B$  can be produced. Finally by averaging  $am$ -values taken from the  $f = 0$  curve corresponding to each of the "fine-scale" values of  $\alpha$ , synthetic curves can be constructed showing the average  $am$ -index for given  $\cos\alpha$  and given  $f$ . The results are qualitatively very similar to what is shown in Figures 13 through 15. By assuming that the variability of the north-south component is considerably greater than that of the other components of the magnetosheath field one can even obtain reasonable quantitative agreement.

As our knowledge of fluctuations of the field in the magnetosheath - that turbulent layer between the bow-shock and the magnetopause - is rather limited (e.g., Fairfield, 1976) it is not possible at the present to extend the simulations mentioned above to more realistic conditions, but it already seems likely that most - if not all - of the difference between the dependence of  $am$  on  $\cos\alpha$  for different degrees of varia-

bility can be understood simply in terms of averaging the non-linear response of  $a_m$  to  $\cos\alpha$  over varying amounts of variance. It does not seem necessary to invoke any ideas that the variance *per se* is instrumental in producing geomagnetic activity. As a matter of fact, as is evident from Figure 14, for southwards fields, activity actually *decreases* with increasing variability of the field.

The relative variability,  $f$ , is typically near 0.5. In Figure 16 we have plotted the value of reduced  $a_m$ -index as a function of  $\cos\alpha$  for several values of  $f$  near 0.5. The scale for  $a_m$  is logarithmic and the resulting nearly linear trends of the datapoints suggest a simple exponential relation

$$a_m = k(f)e^{-g(f)\cos\alpha} \quad (4)$$

where  $k$  and  $g$  vary slightly with  $f$ . Within the typical range of  $f$  we may consider  $g$  to approximately constant, being near  $3/4$ . Although such an empirical relation is very convenient to work with, we should emphasize that it is just that and that it not immediately implies physical reality or insight. The value of  $k$  follows from Figure 14 by setting  $\cos\alpha$  equal to zero.

#### 6. COMPUTATION OF THE AM-INDEX FROM SOLAR WIND DATA

Statistically, the variability, the field magnitude, and the plasma density all depend slightly on the solar wind speed. Figure 17 shows the average relative variability as a function of  $V$ . A similar increase with  $V$  is found on the average for the field strength,

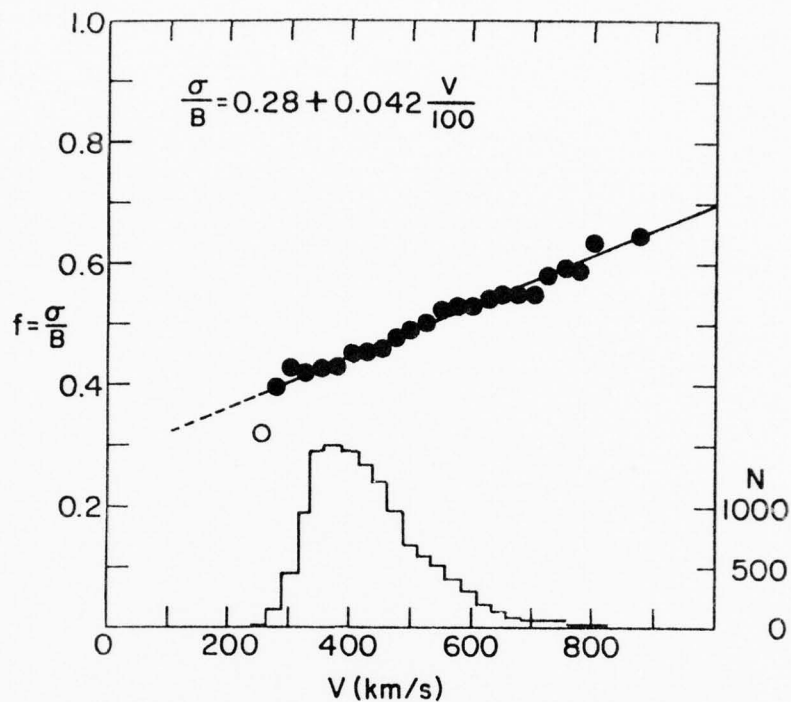


Figure 17. Average value of the relative variability  $f = \sigma/B$  of the interplanetary magnetic field as a function of solar wind speed  $V$ , computed for 25 km/s bins. The histogram shows the number of three-hour intervals in each bin. A linear relation  $f = 0.28 + 4.2 \times 10^{-4}V$  fits the data. Over the observed range of  $V$ , a power-law:  $f \propto V^{0.4}$  is an equally good fit. Dividing the data into two parts:  $dV/dt > 0$  and  $dV/dt < 0$  gives essentially the same result for each partition except that  $f$  is 10% higher for the subset with increasing velocity than for the subset with decreasing speed. A similar result holds for the field magnitude  $B$  although somewhat more noisy.

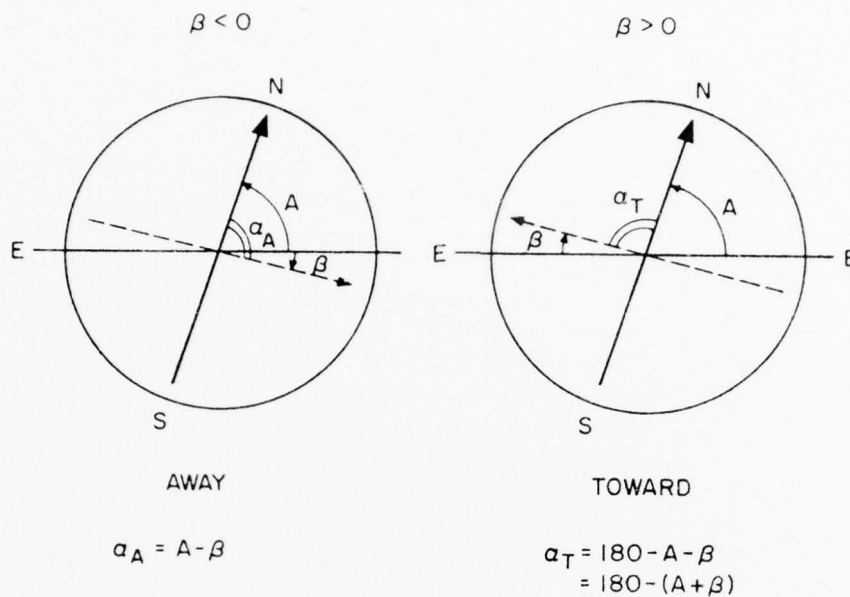


Figure 18. Field line geometry at the nose of the magnetosphere as seen from the sun for different orientations of the interplanetary magnetic field (dashed arrow) and the geomagnetic field (solid arrow marked SN). The ecliptic is indicated by EE. The interplanetary field is assumed to be "draped" around the nose of the magnetosphere as shown in Figure 3. This means that away-polarity is directed from dawn to dusk (left panel) and toward polarity is directed from dusk to dawn (right panel). The angle A is the angle between the geomagnetic field lines and the ecliptic measured from the ecliptic towards the field lines and varying from 55 to 125 depending on season and on universal time.  $\beta$  is the latitude angle of the interplanetary field. The angle  $\alpha$  between the two fields is now defined as shown separately for the two polarities.

while the density is anti-correlated with  $V$ . For the range of  $V$  from 250 km/s to 850 km/s all these relationships can be approximated with power-laws:

$$f \sim V^{0.4}, k \sim V^{0.25}, B \sim V^{0.4}, n \sim V^{-0.5} \quad (5)$$

Combining (2) through (5) under typical conditions ( $\cos \alpha = 0$ ) we get that the am-index should depend on solar wind speed approximately as

$$am \sim BV(nV^2)^{1/3} \cdot k \sim V^{2.15} \quad (6)$$

We may compare this result with Figure 5 and note reasonable agreement.

We have thus found that the rather simple statement that geomagnetic activity increases roughly with the square of the solar wind speed does not reflect an equally simple physical situation but is a consequence of several physical and statistical conditions cooperating in a rather complex manner. The major contributions arise from the BV-factor and from the momentum flux factor ( $nV^2$ ) to the one-third power. The physics of the specific way the momentum flux or the dynamic pressure of the solar wind enters into the functional expression for geomagnetic activity such as eq.(2) is not well understood. The same is the case with the details of magnetic reconnection or plasma cross-field diffusion. On the other hand, we have obtained a rather detailed understanding - or at least a quantitative description - of how solar wind parameters affect the geomagnetic field on the larger scale. The degree to which we can reproduce the observed am-index from solar wind data may be judged from Figure 19 which shows for a number of Bartels rotations both observed and reconstructed am-indices. The comparison

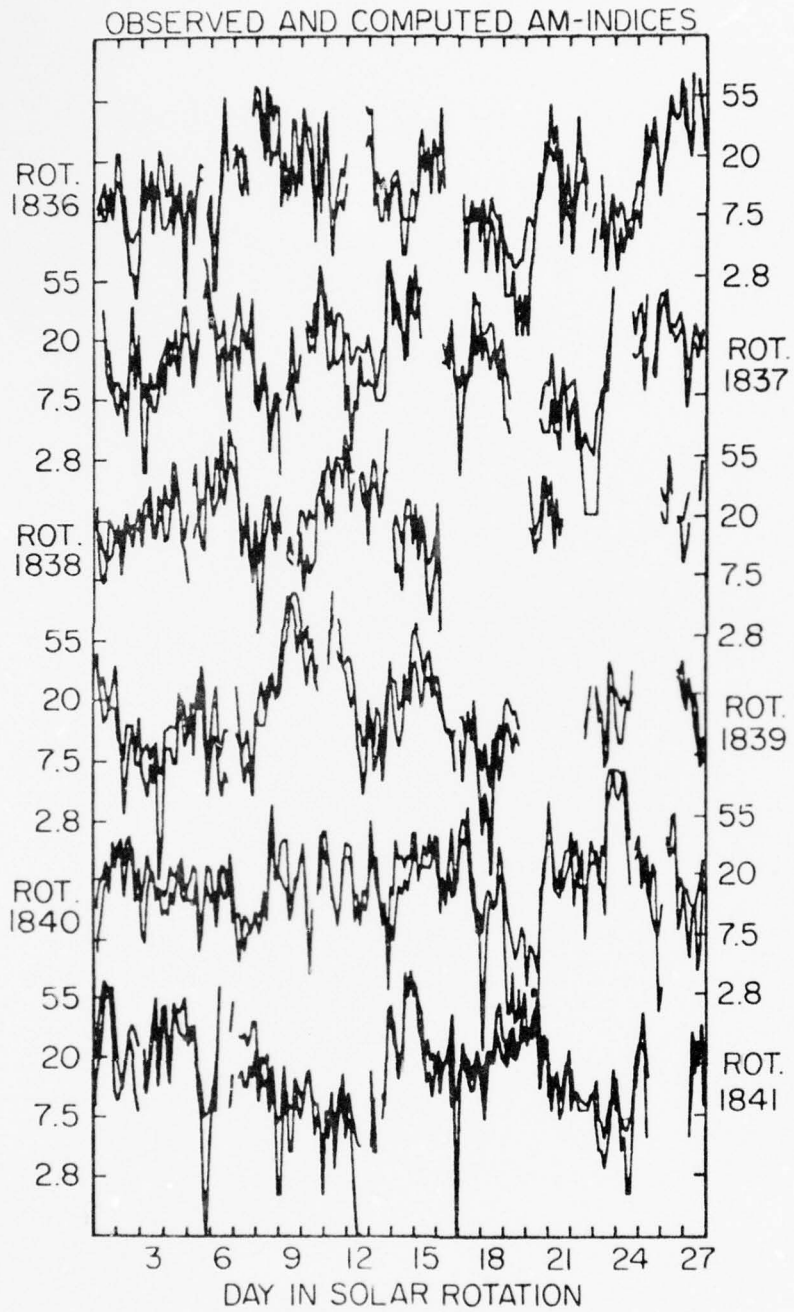


Figure 19

Figure 19. Observed and reconstructed am-indices for Bartels rotations 1836-1841 (Oct. 3, 1967 to March 12, 1968). For every three-hour interval where solar wind data was available, am was computed using

$$am = 6.6 q(f, \alpha) \left\{ \frac{BV_0}{21} \right\} \left[ \frac{nV_0^2}{105} \right]^{1/3} \frac{1.157}{(1+3\cos^2\psi)^{2/3}}$$

where  $V_0 = V/100$  ( $V$  is solar wind speed in km/s),  $B$  is field magnitude in nT, and  $n$  is the number density in protons per  $\text{cm}^3$ . The function  $q(f, \alpha)$  of relative variability  $f$  and angle  $\alpha$  is the fit to reduced am given in the caption to Figure 15. The scale of am is logarithmic because we want to verify the synthesized am-indices against observations over the full range of the index rather than just for the higher values of the index. The two overlapping curves show the two indices for times when solar wind data was available. Where only a single curve is visible over a certain time interval it just means that the computed and the observed indices track each other perfectly. The main area of disagreement is for very small am-values ( $am \leq 1$ ; all such cases are plotted as  $am=1$ ).

Figure 20. a) Computed values of  $\cos(A-\beta_+)$  for each three-hour interval of every month. The result is presented as a contourplot (negative contours are dashed). The angle  $A$  depends on day of year and on Universal Time. Let  $\lambda$  be the ecliptic longitude of the mean sun and let  $d$  denote day of year (Jan. 1  $\equiv$  1). We then have the following approximate relations for computation of  $A$ :

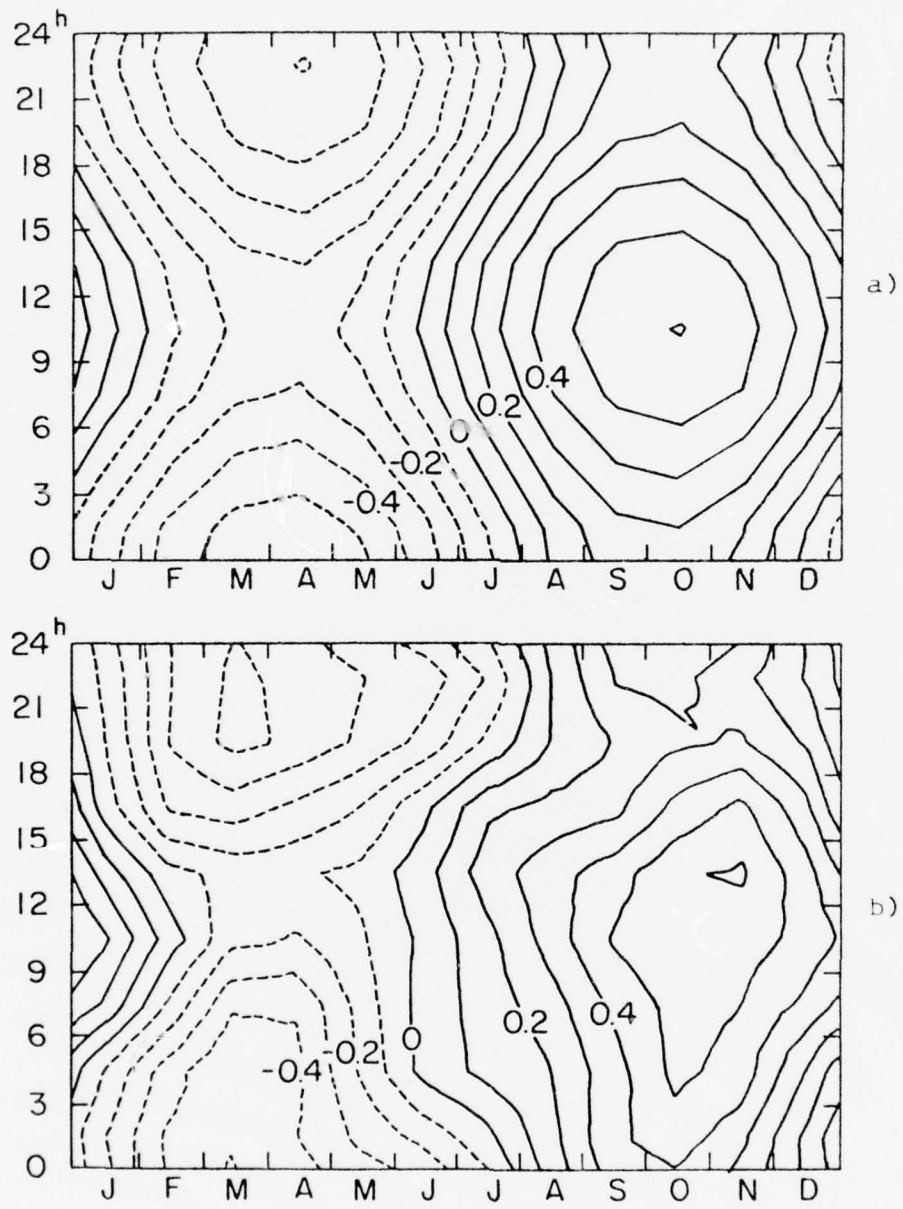


Figure 20

(Figure 20, continued)

$$\lambda(d) = 279^{\circ}69 + 360^{\circ}/365.24 (d - \frac{1}{2})$$

$$h(UT) = 360^{\circ}/24 (UT - 10^{\text{h}}40^{\text{m}}) + \lambda$$

$$\cos\psi = \sin\lambda\cos i\sin\epsilon - \sin i(\sin\lambda\cos\epsilon\cosh - \cos\lambda\sinh)$$

$$\cos\chi = \cos\lambda\cos i\sin\epsilon - \sin i(\cos\lambda\cos\epsilon\cosh + \sin\lambda\sinh)$$

and finally

$$\cos A = \cos\chi / \sin\psi$$

$\epsilon = 23^{\circ}5$  is the obliquity of the ecliptic and  
 $i = 11^{\circ}5$  is the geographical co-latitude of the  
earth's magnetic pole.

b) Observed yearly and Universal Time variation  
of

$$\delta(t) = 2 \cdot (\overline{am}_{\text{Away}} - \overline{am}_{\text{Toward}}) / (\overline{am}_{\text{Away}} + \overline{am}_{\text{Toward}})$$

for the interval 1963-1974 when interplanetary mag-  
netic field data was available. For each month  
and every three-hour UT-interval we find the aver-  
age values of the am-index separately for *Away* po-  
larity and for *Toward* polarity. More precisely,  
the sign of the azimuthal component of the inter-  
planetary magnetic field has been used as the se-  
lection criterion ( $B_Y \geq 0 \equiv \text{Away}$ ;  $B_Y < 0 \equiv \text{Towards}$ ) be-  
cause it is this component that controls the way  
the interplanetary magnetic field is draped around  
the nose of the magnetosphere (see Figure 3).

A slight smoothing of the data has been performed  
by the contour plotting routine.

is quite satisfactory over the full range of activity from quiet to very disturbed. Similar comparisons have been carried out for the entire sunspot cycle with the same satisfactory result. The main area of disagreement seems to be for extremely quiet intervals (*e.g.*,  $a_m = 0$ ) where the reconstructed values turn out a little too high - typically about 2 rather than 0. Possibly the curves for  $\cos \alpha$  near +1 in Figure 14 should be lowered somewhat or maybe the  $a_m$ -index is a poorer measure of geomagnetic activity for very small values of the index where it is extremely difficult to measure.

#### 7. SEMI-ANNUAL AND UNIVERSAL TIME VARIATIONS

The usefulness of the concept of the earth being a probe for interplanetary and solar conditions depends on our understanding of the "instrumental response function". The foregoing analysis suggests that we have reached a point where physically meaningful quantitative results can be extracted from geomagnetic data. Let us consider an idealized interplanetary magnetic field configuration. The field is wound by solar rotation into a spiral in the equatorial plane of the sun. Because the ecliptic is inclined  $7\frac{1}{4}^{\circ}$  to the solar equator the ecliptic latitude angle of the average interplanetary magnetic field measured at the earth vary with time of year:

$$B_p = -p B_0 \cos t \quad (7)$$

where  $B_0 = 7.25$  and  $t$  is reckoned from 0 to  $2\pi$  from December 7 when the heliographic latitude of the earth is zero. Note that for the two opposite polarities of the field  $B$  has opposite signs ( $p = +1$  =

polarity away from the sun;  $p=-1$   $\equiv$  polarity towards the sun). If  $A$  is the angle between the ecliptic and the geomagnetic field lines at the nose of the magnetosphere (see Figure 18), then

$$\alpha_+ = A - \beta_+ \quad , \quad \alpha_- = 180^\circ - (A + \beta_-) \quad (8)$$

thus

$$\cos \alpha_- = -\cos(A + \beta_-) = -\cos(A - \beta_+) = -\cos \alpha_+ \quad (9)$$

Using eq.(4) we may now compute the expected average value,  $\bar{a}$ , of geomagnetic activity assuming equal probability of both polarities:

$$\begin{aligned} \bar{a}(t) &= \frac{1}{2}(a_+ + a_-) = \frac{1}{2}k(e^{-g \cos \alpha_+} + e^{+g \cos \alpha_+}) \\ \bar{a}(t) &= k \cdot \cosh(g \cos(A - \beta_+)) \end{aligned} \quad (10)$$

Similarly, we get for the difference in activity between the two polarities

$$\Delta a(t) = a_+ - a_- = -2k \cdot \sinh(g \cos(A - \beta_+)) \quad (11)$$

The ratio  $\delta(t) = \Delta a(t) / \bar{a}(t)$  is independent of  $k$  and depends only on the geometry of the situation

$$\delta(t) = -2 \cdot \tanh(g \cos(A - \beta_+)) \quad (12)$$

Because  $g \cos(A - \beta_+)$  is always numerically less than 0.5 we may write

$$\delta(t) = -2g \cdot \cos(A - \beta_+) \quad (13)$$

In Figure 20a we show the variation of  $\cos(A - \beta_+)$  with time  $t$ , computed for each three-hour UT-interval of every month of the year; and in Figure 20b we show for comparison the observed variation of  $\delta(t)$ . The agree-

ment is quite good with respect to phase; the amplitudes of the variations shown in the figure are very nearly the same, corresponding to a value of  $2g$  of unity, or  $g = 0.5$ . This is somewhat smaller than the 0.75 found earlier using individual three-hourly observations rather than assuming an ideal field configuration. In fact we get here a measure of the error committed by working with the idealized field instead of the actual field orientation.

The Universal Time variation of  $\delta(t)$  has a maximum at  $10^{\text{h}}30^{\text{m}}$  UT and a minimum at  $22^{\text{h}}30^{\text{m}}$ , while the yearly variation has a minimum in early April and a maximum in early October. The amplitudes of these changes are very substantial amounting to 60% attesting to the strong control of the activity by the field orientation. Because  $\cosh(x) = \cosh(-x)$ , eq.(10) predicts a semi-annual variation of  $\bar{a}(t)$  as was first realized by Russell and McPherron (1973), but this variation is of insignificant amplitude and is almost completely masked by another semiannual variation related to the dipole tilt angle (*e.g.*, Berthelier, 1976). Figure 21 is contourplots of observed average am-index in the same format as used in Figure 20. Furthermore, high activity is indicated by dotted regions and is predominantly observed near the equinoxes. The amplitude of the observed variation is three times larger than that predicted by eq.(10) and the phase is very different. Eq.(10) predicts maxima at times when  $\delta(t)$  attains extremum values (*c.f.* Figure 20) quite contrary to the observed phase of the average am-variation (*c.f.* Mayaud, 1974a). We are then forced to concede that a further modulation of geomagnetic activity exists producing the variations shown in Figure 21b and the dif-

ference between the two lines in Figure 12. As first suggested by Bartels (1925) it seems that geomagnetic activity is enhanced when the earth's dipole axis is perpendicular to the solar wind direction. That we are dealing with a modulation rather than an excitation mechanism is suggested by the basically parallel lines in Figure 12 showing that the influence of the dipole tilt is proportional to the level of activity itself.

---

Figure 21. a) Contourplot computed from eq.(16) with  $am_0$  set equal to the average value of  $am$  over the 1959-1974 period (see below).

b) Contourplot of the observed variation of the  $am$ -index with time of year and with Universal Time. The observed variation is based on 16 years of data (1959-1974). Regions of maxima are dotted. The first full contourline corresponds to  $am = 21$ , and lines are drawn one  $am$ -unit apart. Contour lines in regions of lower than average values are shown as dashed lines.

The correlation between the two contour plots is 0.90, *i.e.* a) is a very good fit to b).

In this figure no separation according to polarity has been performed so we should have a plot of the quantity  $\bar{a}(t)$ , *i.e.* activity averaged over both polarities. Note that the UT-variations for the two solstices are in anti-phase and that the UT-variation at the equinoxes is small with two maxima and two minima during the UT-day. Other magnetic indices (*e.g.*,  $K_p$  or AE) show similar yearly variations but very distorted UT-variations due to uneven station distributions.

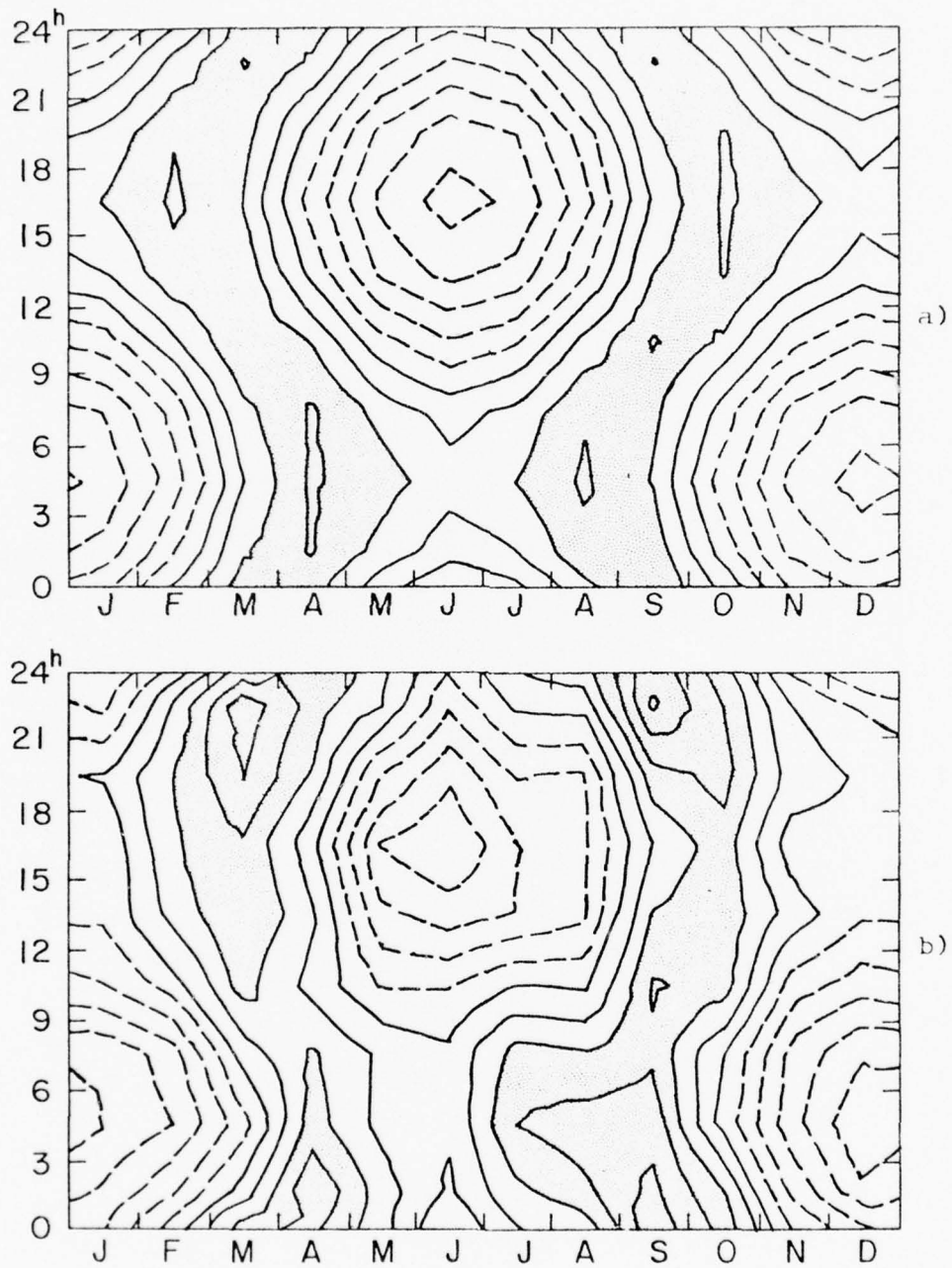


Figure 21

The physical explanation for the dipole tilt modulation of activity is still obscure. It has been suggested (Boller and Stolov, 1970; Mayaud, 1977) that the Kelvin-Helmholtz instability of the boundary between two magnetohydrodynamic fluids in relative motion may be operating at the flanks of the magnetosphere leading to release of some of the energy stored in the magnetotail. An approximate instability criterion may be expressed as

$$M_A^2 > 1 + (B_i/B_o)^2 \cos^2 \psi \quad (14)$$

where  $B_o$  and  $B_i$  are the magnetic field strengths just outside and just inside the magnetopause. If the Alfvénic Mach-number  $M_A = (\text{solar wind speed})/(\text{Alfvén speed})$  exceeds some value depending on the angle  $\psi$  between the solar wind direction and the dipole axis then the magnetopause may be unstable against the growth of the Kelvin-Helmholtz instability, thereby maybe resulting in a greater stress on the magnetosphere.

It is also possible that the coupling between the solar wind and the magnetosphere is dependent on the basic geometry of the magnetic field around a dipole:

$$B = B_{eq} (1 + 3\cos^2 \psi)^{1/2} \quad (15)$$

where  $B_{eq}$  is the field strength in the equatorial plane. In any case, the parameter  $(1+3\cos^2 \psi)$  has been found to enter into a simple empirical expression for the modulation, namely

$$am = 1.157 am_0 (1 + 3\cos^2 \psi)^{-2/3} \quad (16)$$

which produces an excellent fit to the observed am-variation with  $\psi$ . Figure 21a shows the variation of the above relation with time of year and time of UT-

day. The constant 1.157 is just a normalization factor (equal to the yearly mean value of  $(1+3\cos^2\psi)^{2/3}$ ) and  $am_0$  is the unmodulated value of  $am$ . Of course, the relation given by eq.(16) is not unique, but there can be little doubt that some function of  $\psi$  accounts for the observed variations in considerable quantitative detail. This result puts an upper limit on systematic variation of solar wind speed with heliographic latitude. Judging from Figure 21, it seems that no more than two  $am$ -units ( $nT$ ) are not already accounted for. This corresponds to about 10%. Referring to Figure 5, we can translate that into a maximum variation with heliographic latitude of the wind speed of 16 km/s over 7 degrees of latitude, or 2.3 km/s per degree. Any variation larger than that would distort the variation shown in Figure 21 in an unacceptable way.

#### 8. VARIATIONS WITH HELIOGRAPHIC LATITUDE

In a careful analysis of a 100-year series of the geomagnetic activity index  $aa$ , Mayaud (1974b) showed that the semi-annual variation attains maxima  $4.0 \pm 2.5$  days after the equinoxes. This difference can be understood in terms of the aberration of the solar wind caused by the earth's orbital movement. A significant variation of solar wind speed with heliographic latitude would shift the time of maxima towards March 7 and September 7 when the earth is at the highest latitudes. No such shifts are observed when activity series of sufficient length are analyzed. If high-speed solar wind streams predominantly originate in coronal holes that are lower-

latitude extensions of the polar holes ("polar cap lobes") one would naturally expect at least a statistical tendency for solar wind speed to be higher at higher heliographic latitudes. The situation is analogous to the classical axial-equinoctial controversy among students of terrestrial magnetism. The axial explanation of the semiannual variation takes its starting point in the fact that sunspots occur most frequently in heliographic latitudes higher than  $10^{\circ}$  while the equatorial belt of the sun is relatively free of spots. If, then, the solar wind streams originate in the same belts in which the spots occur they should more likely sweep across the earth in March and September causing an enhancement of geomagnetic activity at those times of the year. This explanation is very simple and intuitively appealing in contrast to the equinoctial hypothesis that ascribes the enhancement to an obscure and largely unspecified mechanism whose efficiency is somehow - in an unknown way - modulated by the angle between the geomagnetic dipole and the solar wind flow direction. Today - as forty-five years ago (Bartels, 1932) - the axial hypothesis must be discarded because of its discordance with observations. Direct *in-situ* observations of solar wind speed (Bame *et al.*, 1977) and of interplanetary magnetic field strength (King, 1976) over one full sunspot cycle show indeed no detectable variation of either parameter with heliographic latitude within  $\pm 7^{\circ}$  of the solar equator.

Such a variation is, however, found in the polarity of the interplanetary magnetic field. Rosenberg and Coleman (1969) found that the probability of occurrence of a given polarity in a 27-day solar rotation varies

in a roughly sinusoidal way during the year in phase with the heliographic latitude of the observer (at or near the earth). Wilcox and Scherrer (1972) extended the analysis back in time to cover more than four sunspot cycles and showed that the phase of the above 'Rosenberg-Coleman' effect reverses 2-3 years after each sunspot maximum coinciding with the inferred times of reversals of the solar polar fields. The Rosenberg-Coleman effect owes its existence to the fact that the interplanetary magnetic field within several astronomical units of the sun appears to have one polarity in most of the hemisphere north of the solar equatorial plane and the opposite polarity in most of the hemisphere south of the equatorial plane (Svalgaard and Wilcox, 1976; Smith *et al.*, 1977). The two hemispheres are separated by a warped or curved current sheet that typically crosses the solar equatorial plane in 2 to 4 places, thus dividing the equatorial region into 2 to 4 sectors of alternating polarity. Near sunspot minimum the latitudinal extent of the warps of the curved current sheet is of the order of  $10^{\circ}$ , so that the sector boundary (*i.e.*, the current sheet separating the two hemispheres of opposed field polarity) is almost parallel to the solar equatorial plane. It is then clear that at such times going out of the solar equatorial plane will increase the probability of observing a certain polarity over that of observing the opposite polarity. If the observer reaches a latitude greater than the extents of the sector-warps in the current sheet, he will see a unipolar interplanetary magnetic field with no sector structure at all (Smith, *et al.*, 1977).

## 9. THE 22-YEAR CYCLE IN GEOMAGNETIC ACTIVITY

Let us model the Rosenberg-Coleman effect with an expression of the form:

$$w_p = \frac{1}{2} + p \cdot r \cdot \sin t \quad (17)$$

where  $w_p$  is the probability of observing the polarity  $p$ . Time  $t$  varies from 0 to  $2\pi$  during the course of a year and is reckoned from December 7 when the heliographic latitude of the earth is zero. The magnitude of the coefficient  $r$  depends essentially on the latitudinal extent of the warps in the sector boundary current sheet, while the sign of  $r$  changes when the polarity of the solar poles reverse shortly after each sunspot maximum. Figure 22 shows the value of  $r$  as a function of the warping of boundary.

Geomagnetic activity averaged over both polarities may now be written

$$a(t) = w_+ a_+ + w_- a_- = \frac{1}{2}(a_+ + a_-) + r(a_+ - a_-) \sin t$$

$$a(t) = \bar{a}(t)(1 + r\delta(t)\sin t) \quad (18)$$

In order to simplify the considerations we will work with daily averages so that the Universal Time variation of  $\delta(t)$  is averaged out. In that case we find that  $\delta(t)$  varies very nearly sinusoidal during the year but with a phase that is different from the phase of the heliographic latitude variation. Let the phase difference be  $\eta$  ( $\eta \approx 33^\circ$ ) then from eq.(13) and Figure 20:

$$\delta(t) = -2g \cdot 0.43 \sin(t + \eta) \quad (19)$$

Averaged over a full year  $\sin(t)\sin(t+\eta)$  is equal to  $\frac{1}{2}\cos\eta$  so that the yearly average of  $a(t)$  can be written

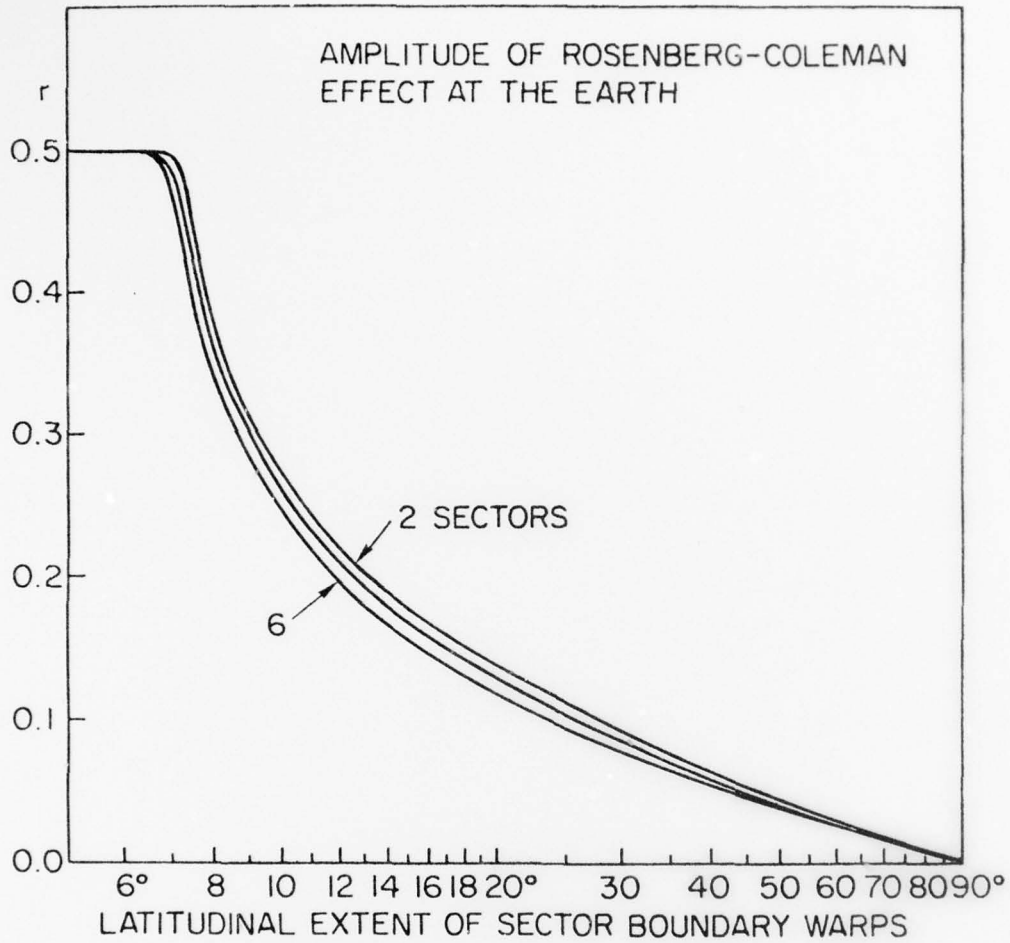


Figure 22. Amplitude,  $r$ , of the Rosenberg-Coleman effect at the earth as a function of latitudinal extent of the curved current sheet that separates opposite field polarities in interplanetary space (see text for definition of  $r$ ). The number of sectors per rotation (2, 4, or 6) has a slight influence on  $r$  as shown. Computation of  $r$  was done here by a simple computer simulation of the geometrical situation.

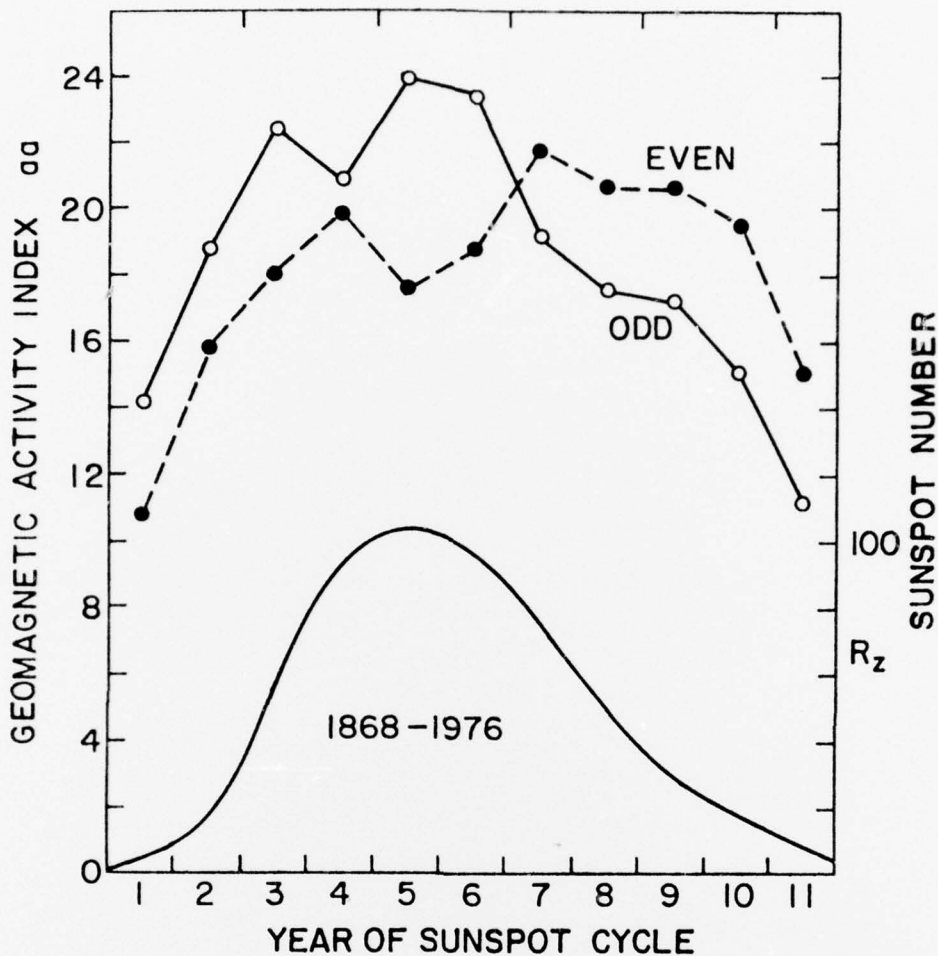


Figure 23. Variation of yearly means of geomagnetic activity as a function of phase within the sunspot cycle. Activity is measured by the aa-index which for this purpose can be considered identical to the am-index. Even-numbered (filled circles) and odd-numbered (open circles) cycles are considered separately. At the bottom is shown the average sunspot numbers for the solar cycles since 1868 when the aa-series begins. Note that during the first half of the cycle, odd cycles are more geomagnetically active than even cycles while the reverse is true during the last half of a sunspot cycle.

$$\langle a \rangle_{\text{year}} = \langle \bar{a} \rangle (1 - 0.43gr \cdot \cos n) = \langle \bar{a} \rangle (1 - 0.28r) \quad (20)$$

Thus for the eleven years - from shortly after one sunspot maximum to shortly after the next - when  $r$  is negative geomagnetic activity will be increased, while for the next eleven years when  $r$  is positive activity will be diminished. This 22-year cycle in geomagnetic activity is actually observed (Chernosky, 1966; Russell, 1974) as shown in Figure 23, depicting the average sunspot cycle variation of geomagnetic activity shown separately for odd- and even-numbered sunspot cycles.

If we set  $r = 0.25$ , corresponding to a maximum sector boundary warp of  $10^0$ , the difference in activity between odd and even cycles should be about 14% according to eq.(20) to be compared with the 20% actually observed. Considering the many simplifications we have introduced, the agreement is quite satisfactory. The 22-year cycle is a good example of how geomagnetic measurements can be a valuable supplement to direct observations of the sun -- polar field reversals have only been directly observed twice.

#### 10. VARIATIONS OF GEOMAGNETIC DISTURBANCES WITH SOLAR ACTIVITY

When it was thought that geomagnetic activity was caused by corpuscular streams emitted from active regions on the sun (either sunspots or facular areas), the sunspot cycle variation of geomagnetic activity was taken for granted, as something that hardly required any elaboration. Today, the primary effect of solar activity is generally believed to be caused by compression of the

ambient solar wind by blastwaves emitted from solar flares. The ensuing high values of solar wind speed, density and especially magnetic field strength ensure major events of violent activity: geomagnetic storms which have an obvious sunspot cycle dependence. But, in addition, variations of fundamental solar wind parameters can be very important. The 1973-75 period resulted in exceptionally high geomagnetic activity to the extent that it is hard to speak about a regular sunspot cycle variation of geomagnetic activity for the period 1965-1976. In a similar way solar wind speed has had a pronounced tendency to have higher values in the years preceding sunspot minimum ever since spacecraft data became available in the early 1960's (Gosling *et al.*, 1976; Bame *et al.*, 1977). On the other hand, no sunspot cycle related variation of magnetic field magnitude has been found (King, 1976). In order to put the recent data in proper perspective it is necessary to consult the historical record. Geomagnetic activity has been monitored for almost two centuries and reliable indices of constant calibration exist for little longer than the past one hundred years. As shown in Figure 24, very significant long-term trends exist in the activity record. The sunspot cycle variation is generally discernible in addition to a variation on a time scale of 80-100 years. It is interesting that the last sunspot cycle is not at all typical (although maybe #16 from 1924 to 1933 is somewhat similar to cycle #20). We should, therefore, exercise caution in drawing general conclusions about the sunspot cycle behavior of the solar wind parameters from observations covering only the last cycle.

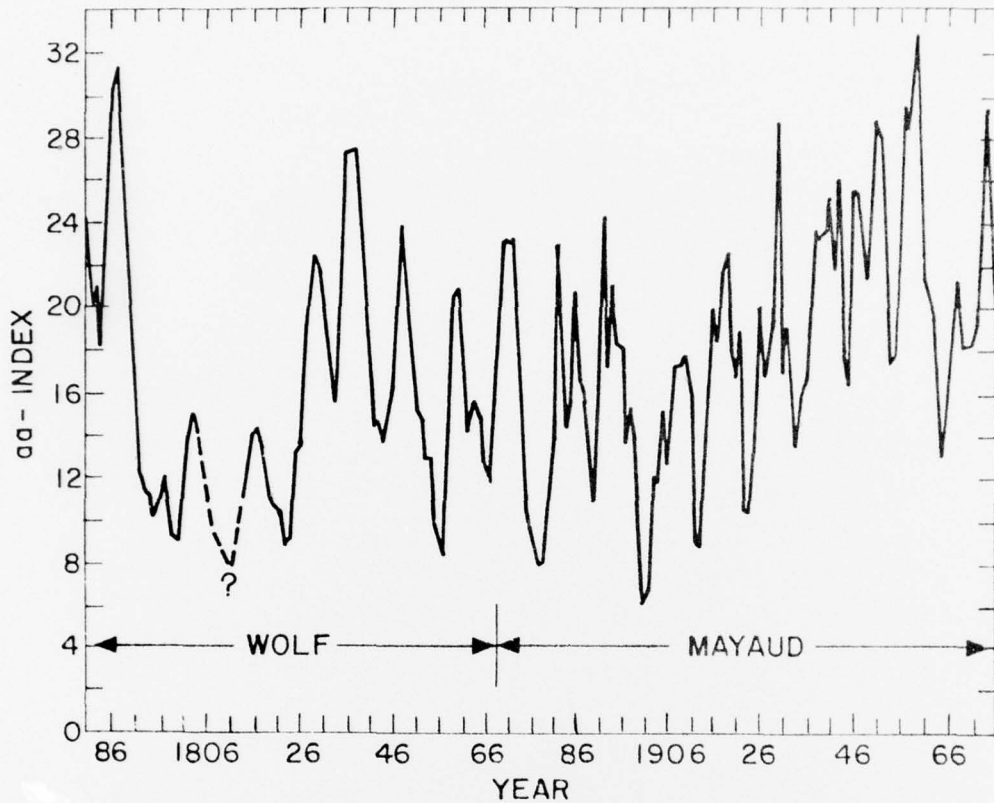


Figure 24. Yearly means of geomagnetic activity from 1781 to the present. From 1868 the index is homogeneous and has constant calibration as discussed by Mayaud (1972). The earlier data has been derived from the daily ranges of magnetic declination as given by Wolf (1884). This earlier series covers the interval 1781 through 1880. For the interval 1868-1880 the two series overlap, permitting a cross-calibration of Wolf's index in terms of the aa-index. No magnetic data is available for 1805-1813 so Wolf used yearly counts of auroral displays and calibrated them in terms of magnetic activity. Finally, Wolf wanted to emphasize the sunspot cycle variation of geomagnetic activity and had smoothed his index to remove short-term fluctuations (though he ends up reporting monthly values!).

Since the year 1900 the general level of geomagnetic activity has increased at least two-fold even to the extent that the activity at recent sunspot minima exceeds that of the sunspot maximum of 1906. It seems likely that either the average solar wind speed and/or the magnitude of the interplanetary magnetic field has changed significantly over the past 75 years. A general change in solar wind speed entails a corresponding change in field magnitude because of different spiral angle of the interplanetary magnetic field. The product  $BV$  is in fact given by

$$BV = B_R(V^2 + \Omega^2 R^2)^{\frac{1}{2}} \quad (21)$$

where  $B_R$  is the radial component of the field at distance  $R$  and  $\Omega = 2.87$   $\mu$ radian/s is the angular velocity of solar rotation. If  $V$  becomes considerably smaller than  $\Omega R = 430$  km/s at 1 AU, the quantity  $BV$  is almost constant provided that  $B_R$  is constant. The net result is that an overall change in solar wind speed alone changes the am-index according to  $am \sim V$  rather than  $am \sim V^2$ , which means that the decrease by a factor of two in am-index back to 1900 corresponds to a similar decrease of  $V$  from 400 km/s to 200 km/s. It seems more likely to the present author that it is mainly the field magnitude that has changed through a change of  $B_R$  (*i.e.* a change of the open magnetic flux). The sunspot number is presumable some crude measure of the closed magnetic flux and it is not unreasonable to expect a similar trend in the open flux. As seen in Figure 24 the long-term trends in geomagnetic activity since 1781 follows rather closely similar trends in the maximum sunspot numbers in each cycle, suggesting similar trends in available magnetic flux.

It would be very desirable to be able to infer the interplanetary magnetic field strength independently from the solar wind speed from geomagnetic data. Some recent works (Russell and Fleming, 1976; Gul'yel'mi and Bol'shakova, 1973) suggest that the period of certain types of micropulsations of the geomagnetic field (Pc2 to Pc4 with periods from 5 to 150 seconds) is strongly controlled by the magnitude of the interplanetary magnetic field and can in fact be used as a diagnostic for that quantity. No attempt has yet been made to extend the analysis to the pre-satellite era.

## 11. CONCLUSION

In this chapter we have outlined some current ideas about the interaction between the solar wind and the earth's magnetosphere and showed how they can help organize the analysis of how solar wind parameters influence geomagnetic activity. A rather detailed description of the dependence of geomagnetic activity on solar wind conditions is now available and permits conclusions about large-scale and long-term properties of the sun and of the solar wind to be deduced from the geomagnetic records. On the other hand, the discovery of coronal holes seems to have brought us close to the solution of the old problem of a solar identification of the elusive M-regions thought responsible for recurrent sequences of enhanced geomagnetic activity. Thus solar and geophysical research have recently strengthened their links in the important study of the environment of mankind.

#### ACKNOWLEDGEMENTS

This work was supported in part by the Office of Naval Research under Contract N00014-76-C-0207, by the National Aeronautics and Space Administration under Grant NGR 05-020-559, by the Atmospheric Sciences Section of the National Science Foundation under Grants ATM74-19007 and DES75-15664, and by the Max C. Fleischmann Foundation, and was stimulated by the Skylab workshop on coronal holes. I thank J.H.King at the National Space Science Data Center for solar wind plasma and field data. The National Geophysical and Solar-Terrestrial Data Center has provided the geomagnetic activity indices used in the present investigation. I would like to express appreciation of the work carried out at geomagnetic observatories, past and present, all over the world. The continuous recording and careful reduction of geomagnetic variations, sometimes performed under extremely adverse conditions, was started well over a century ago and is today becoming an increasingly important tool of research into solar-terrestrial relations and of the sun itself.

#### REFERENCES

- Bahnsen, A. and A.M. Hansen, Relations between electric fields, currents and plasma in the polar magnetosphere-ionosphere system, *Planet. Space Sci.*, 24, 841, 1976.
- Baker, D.A. and J.E. Hammel, Experimental studies of the penetration of a plasma stream into a transverse magnetic field, *Physics of Fluids*, 8, 713, 1965,
- Baliff, J.R., D.E. Jones and P.J. Coleman, Jr., Further evidence of the correlation between transverse fluctuations in the interplanetary field and  $K_p$ , *J. Geophys. Res.*, 74, 2289, 1969.
- Bame, S.J., J.R. Asbridge, W.C. Feldman, H.E. Felt- hauser and J.T. Gosling, A search for a general gradient in the solar wind speed at low solar latitudes, *J. Geophys. Res.*, 82, 173, 1977.
- Bartels, J., Eine universell Tagsperiode der erdmagnetischen Aktivität, *Meteorol. Z.*, 42, 147, 1925.
- Bartels, J., Terrestrial-magnetic activity and its relation to solar phenomena, *Terr. Magn. Atmosph. Electr.*, 37, 1, 1932.
- Bartels, J., Potsdamer erdmagnetische Kennziffern, *Z. Geophys.*, 14, 68, 1938.
- Berthelier, A., Influence of the polarity of the interplanetary magnetic field on the annual and the

- diurnal variation of magnetic activity, *J. Geophys. Res.*, 81, 4546, 1976.
- Boller, B.R. and H.L. Stolov, Kelvin-Helmholtz instability and the semi-annual variation of geomagnetic activity, *J. Geophys. Res.*, 75, 6073, 1970.
- Burlaga, L.F. and Lepping, R.P., The causes of recurrent geomagnetic storms, Goddard Space Flight Center, *Rep. X-692-76-277*, Greenbelt, Md., Dec. 1976.
- Burton, R.K., R.L. McPherron and C.T. Russell, The terrestrial magnetosphere: A half-wave rectifier of the interplanetary electric field, *Science*, 189, 717, 1975.
- Chernosky, E.J., Double sunspot-cycle variation in terrestrial magnetism 1884-1963, *J. Geophys. Res.*, 71, 965, 1966.
- Cole, K.D., Outline of a theory of solar wind interaction with the magnetosphere, *Planet. Space. Sci.*, 22, 1075, 1974.
- Crooker, N.U., Solar wind-magnetosphere coupling, *Rev. Geophys. Space Sci.*, 13, 955, 1975.
- Crooker, N.U., J. Feynman and J.T. Gosling, On the high correlation between long-term averages of solar wind speed and geomagnetic activity, *J. Geophys. Res.*, 82, (in press), 1977.
- Eastman, T.E., E.W. Jones, Jr., S.J. Bame and J.R. Asbridge, The magnetospheric boundary layer: site of plasma, momentum and energy transfer from the magnetosheath into the magnetosphere, *Geophys. Res. Letters*, 3, 685, 1976.

- Fairfield, D.H., The ordered magnetic field of the magnetosheath, *J. Geophys. Res.*, 72, 5865, 1967.
- Fairfield, D.H., Magnetic fields of the magnetosheath, *Rev. Geophys. Space Phys.*, 14, 117, 1976.
- Garrett, H.B., A.J. Dessler and T.W. Hill, Influence of solar wind variability on geomagnetic activity, *J. Geophys. Res.*, 79, 4603, 1974.
- Gosling, J.T., J.R. Asbridge, S.J. Bame and W.C. Feldman, Solar wind speed variations: 1962-1974, *J. Geophys. Res.*, 81, 5061, 1976.
- Gul'yel'mi, A.V. and O.V. Bol'shakova, Diagnostics of the interplanetary magnetic field from ground-based data on Pc 2-4 micropulsations, *Geomagn. Aeron.*, 13, 535, 1973.
- Holzer, T.E. and Reid, G.C., The response of the day-side magnetospheric ionospheric system to time-varying field line reconnection at the magnetopause 1. Theoretical model, *J. Geophys. Res.*, 80, 2041, 1975.
- King, J.H., A survey of long-term interplanetary magnetic field variations, *J. Geophys. Res.*, 81, 653, 1976.
- Mayaud, P.N., Atlas of indices  $K$ , *IAGA Bull.* 21, 1967.
- Mayaud, P.N., Indices  $K_n$ ,  $K_s$ , et  $K_m$ , 1964-67, *Centre National de la Recherche Scientifique*, Paris, 1968.
- Mayaud, P.N., The aa-indices: a 100 year series characterizing the magnetic activity, *J. Geophys. Res.*, 77, 6870, 1972.
- Mayaud, P.N., Comment on 'Semi-annual variation of geomagnetic activity' by C.T. Russell and R.L. McPherron, *J. Geophys. Res.*, 79, 1131, 1974a.

- Mayaud, P.N., Variation semi-annuelle de l'activité magnétique et vitesse du vent solaire, *C.R. Acad. Sci., Series B*, 278, 132, 1974b.
- Mayaud, P.N., The Boller-Stolov mechanism, and the semi-annual and daily McIntosh effects in geomagnetic activity, *J. Geophys. Res.*, 82, (in press), 1977.
- McIntosh, D.H., On the annual variation of magnetic disturbance, *Phil. Trans. Roy. Soc. Lond., Series A*, 251, 525, 1959.
- Murayama, T. and Hakamada, K., Effects of solar wind parameters on the development of magnetospheric substorms, *Planet. Space Sci.*, 23, 75, 1975.
- Reiff, P.H. T.W. Hill and J.L. Burch, Solar-wind plasma injection at the dayside magnetospheric cusp, *J. Geophys. Res.*, 82, 479, 1977.
- Rosenberg, R.L. and P.J. Coleman, Jr., Heliographic latitude of the dominant polarity of the interplanetary magnetic field, *J. Geophys. Res.*, 74, 5611, 1969.
- Russell, C.T. On the heliographic latitude dependence of the interplanetary magnetic field as deduced from the 22-year cycle of geomagnetic activity, *Geophys. Res. Letters*, 1, 11, 1974.
- Russell, C.T. and R.L. McPherron, Semiannual variation of geomagnetic activity, *J. Geophys. Res.*, 78, 92, 1973.
- Russell, C.T. and B.K. Fleming, Magnetic pulsations as a probe of the interplanetary magnetic field: A test of the Borok B index, *J. Geophys. Res.*, 81, 5882, 1976.

- Sabine, E., On periodical laws discoverable in the mean effects of the larger magnetic disturbances, *Phil. Trans. Roy. Soc. London*, 146, 357, 1856.
- Schatten, K.H. and J.M. Wilcox, Response of the geomagnetic activity index Kp to the interplanetary magnetic field, *J. Geophys. Res.*, 72, 5185, 1967.
- Sckopke, N., G. Paschmann, H. Rosenbauer and D.H. Fairfield, Influence of the interplanetary magnetic field on the occurrence and thickness of the plasma mantle, *J. Geophys. Res.*, 81, 2687, 1976.
- Sheeley, N.R., Jr., J.R. Asbridge, S.J. Bame and J.W. Harvey, A pictorial comparison of interplanetary magnetic field polarity, solar wind speed, and geomagnetic disturbances index during the sunspot cycle, *Solar Phys.*, (in press), 1977.
- Siebert, M., Maßzahlen der erdmagnetischen Aktivität, in *Handbuch der Physik*, 49(3), ed. by S. Flügge, p. 206, Springer, New York, 1971.
- Smith, E.J., B.T. Tsurutani and R.L. Rosenberg, Observations of the interplanetary sector structure up to heliographic latitudes 16: Pioneer 11, *J. Geophys. Res.*, 82, (submitted), 1977.
- Snyder, C.W., M. Neugebauer and U.R. Rao, The solar wind velocity and its correlation with cosmic-ray variations and with solar and geomagnetic activity, *J. Geophys. Res.*, 68, 6361, 1963.
- Svalgaard, L., Recalibration of Bartels' geomagnetic activity indices Kp and ap to include Universal Time variations, *J. Geophys. Res.*, 81, 5182, 1976.
- Svalgaard, L. and J.M. Wilcox, Three-dimensional structure of the extended solar magnetic field and the sunspot cycle variation in cosmic ray intensity, *Nature*, 262, 766, 1976.

Wilcox, J.M. and P.H. Scherrer, Annual and solar magnetic cycle variations in the interplanetary magnetic field 1926-1971, *J. Geophys. Res.*, 77, 5385, 1972.

Wolf, R., Einheitliche Deklinations-Variationen, *Astr. Mitt. Zürich*, Nr. 61, 1884.